METEOR-Berichte

Benthic element cycling, fluxes and transport of solutes across the benthic boundary layer in the Peruvian oxygen minimum zone, (SFB 754)

Cruise No. M92

January 05 – February 03, 2013
Callao (Peru) – Callao (Peru)

S. Sommer, M. Dengler, T. Treude

Editorial Assistance:

DFG-Senatskommission für Ozeanographie
MARUM – Zentrum für Marine Umweltwissenschaften der Universität Bremen

2014

The METEOR-Berichte are published at irregular intervals. They are working papers for people who are occupied with the respective expedition and are intended as reports for the funding institutions. The opinions expressed in the METEOR-Berichte are only those of the authors.

The METEOR expeditions are funded by the *Deutsche Forschungsgemeinschaft (DFG)* and the *Bundesministerium für Bildung und Forschung (BMBF)*.

Editor:
DFG-Senatskommission für Ozeanographie
c/o MARUM – Zentrum für Marine Umweltwissenschaften
Universität Bremen
Leobener Strasse
28359 Bremen

Author:
Dr. Stefan Sommer
Marine Biogeochemie
GEOMAR
Wischhofstr. 1-3
24148 Kiel,
Germany

Telefon: +49 431-600 2119
Telefax: +49 431-600 2928
e-mail: ssommer@geomar.de

Citation: S. Sommer, M. Dengler, T. Treude (2014) Benthic element cycling, fluxes and transport of solutes across the benthic boundary layer in the Peruvian oxygen minimum zone, (SFB 754) - Cruise No. M92 – January 05 – February 03, 2013 – Callao (Peru) – Callao (Peru). METEOR-Berichte, M92, 55 pp., DFG-Senatskommission für Ozeanographie, DOI:10.2312/cr_m92

ISSN 2195-8475

Table of Contents

1 Summary

During this cruise a detailed multi-disciplinary research program was conducted at the Peruvian oxygen minimum zone (OMZ) within the framework of the Kiel SFB 754. Investigations were primarily conducted along a depth transect at 12° S. Major aim was to advance understanding of how OMZ´s are maintained and to determine feedbacks of benthic nutrient release on the currently expanding Peruvian OMZ with a major focus on i. variability of benthic nutrient release in response to hydrodynamic forcing and regional differences in bottom water levels of oxygen (O_2), nitrate (NO_3^-), nitrite (NO_2^-), and sedimentary carbon content, ii. diapycnal and advective fluxes of excess dinitrogen (N_2), ammonium (NH_4^+), phosphorous (P), iron (Fe), silicate (Si), and radium isotopes between the benthic boundary layer, and the stratified interior ocean as well as their entrainment into the surface mixed layer and iii. processes involved in the respective benthic N, Fe, and P cycles. To achieve this goal, physical and biogeochemical measurements were conducted in the water column as well as at the sea floor. For investigations in the water column a total of 84 CTD casts, 41 micro-structure CTD, 20 in situ pump and 12 GoFlo deployments were performed. Sediment samples were obtained during 50 multiple corer casts, 12 gravity corers and 10 benthic chamber lander deployments. Furthermore a profiler lander was used to determine in situ microprofiles of O_2, NO_3^- and nitrous oxide (N_2O) in situ. Microprofiles were obtained using glass-microsensors that were pushed into the sediment in 300 µm increments. In order to obtain time series data on the oxygen distribution and the current regime oceanographic moorings were distributed along the 12°S transect in addition to four benthic satellite-landers each equipped with upward looking ADCPs. Lastly, a glider swarm was established at 12°S. These instruments were deployed for the duration of cruise M92 as well as for the subsequent M93 cruise. Deviating from the cruise proposal, more time was spent for station works at the depth transect at 12° S. Major aim of this cruise was to obtain a coherent data set of all involved groups, which however took slightly more time than originally planned, yet bears a high scientific potential. Additionally, it was discovered that at 12° S in shallow waters sulphide was released from the seabed into the bottom water. Furthermore, in water depths from about 120 to 200 m nitrite in addition to nitrate was available in high concentrations which affects the benthic nitrogen cycle to a hitherto unknown extent. Hence these stations were more intensely investigated than originally planned. Weather conditions were fine and all deployments of the scientific gear went very well. It is expected that after analyses and synthesis of the different data sets from the different disciplines the scientific questions above can be addressed to broad extent.

Zusammenfassung

Im Rahmen des Kieler SFB 754 wurde während dieser Forschungsreise ein multi-disziplinäres Forschungsprogramm in der peruanischen Sauerstoffminimumzone (SMZ) durchgeführt. Die Arbeiten fanden vorwiegend entlang eines Tiefenschnitts bei 12°S statt. Hauptzielsetzung dieser Reise war es unser Verständnis zur Aufrechterhaltung von SMZen zu erweitern und die Auswirkung von benthischen Rückkoppelungsmechanismen auf die sich gegenwärtig ausbreitende peruanische SMZ zu erfassen. Im Vordergrund der Untersuchungen stand i. die Variabilität der benthischen Rückführung von Nährstoffen in Abhängigkeit des hydrodynamischen Regimes sowie regionalen Unterschieden in der Bodenwasserkonzentration

von Sauerstoff (O_2), Nitrat (NO_3^-), Nitrit (NO_2^-), sowie dem Gehalt von organischem Kohlenstoff in den Oberflächensedimenten; ii. die Erfassung von diapyknischen und advektiven Flüssen von Stickstoff (N_2), Ammonium (NH_4^+), Phosphor (P), Eisen (Fe), Silikat (Si) sowie von Radiotracern entlang der benthischen Grenzschicht in die geschichtete Wassersäule und der durchmischten Oberflächenschicht; und iii. Erfassung von Prozessen, die am benthischen Umsatz von N, Fe und P beteiligt sind. Um diese Zielsetzungen zu erreichen, wurde ein umfangreiches physikalisches und biogeochemisches Messprogramm sowohl in der Wassersäule als auch am Meeresboden durchgeführt. Das Arbeitsprogramm in der Wassersäule umfasste insgesamt 84 CTD-, 41 Mikrostruktur CTD-, 20 in situ Pumpen- und 12 GoFlo Einsätze. Sedimentproben wurden mittels 50 Multicorer-, 12 Schwerelot- und 10 Lander Einsätzen erhalten. Zusätzlich wurden 6 Profiler Lander Einsätze zur Erfassung von NO_3^-, Distickstoffmonoxid (N_2O) und O_2 durchgeführt. Zur Zeitserienerfassung von O_2, Strömung und physikalischer Parameter wurden Verankerungen entlang des Tiefenschnitts bei 12° ausgebracht. Diese Messungen wurden durch benthische Satelliten Lander und einen Glider Schwarm ergänzt. Diese Instrumente kamen für die Dauer der Reise M92 als auch für die nachfolgende Fahrt zum Einsatz. Abweichend vom Fahrtantrag wurde mehr Arbeitszeit bei 12° S verbracht. Dies ist darauf zurückzuführen, dass ein koherenter Datensatz aller beteiligter Gruppen bei 12°S gewonnen werden sollte, was mehr Zeit in Anspruch nahm, jedoch ein hohes wissenschaftliches Potential in sich birgt. Ferner zeigte sich beim 12° S Schnitt, dass in den flachen Bereichen Schwefelwasserstoff ins Bodenwasser abgegeben wurde. Weiterhin wurde festgestellt, dass in Wassertiefen von ca. 120 bis 200 m Nitrit zusätzlich zu Nitrat in hohen Konzentrationen verfügbar war und damit in bisher ungekanntem Ausmaß in den benthischen Stickstoffkreislauf eingreift. Deshalb wurden diese Stationen intensiver wie ursprünglich geplant untersucht. Die Einsätze verliefen auch aufgrund der hervorragenden Wetterbedingungen hervorragend, somit steht das angestrebte Datenmaterial zur Verfügung. Abweichend vom Es ist zu erwarten, dass die wissenschaftlichen Fragestellungen zu einem breiten Umfang adressiert werden können. Hierbei liegt in der Synthese der Datensätze verschiedener Fachdisziplinen ein hohes wissenschaftliches Potential.

2 Participants

Name	Discipline	Institution
Sommer, Stefan, Dr.	Benthic Fluxes / Chief Scientist	GEOMAR
Bicking, Seabastian	Benthic fluxes	GEOMAR
Bourbonnais, Annie, Dr.	N-Geochemistry	UMASS
Breitbarth, Eike, Dr.	Fe-Geochemistry	GEOMAR
Cherednichenko, Sergiy	Technician Lander	GEOMAR
Dale, Andy, Dr.	Porewater Geochemistry	GEOMAR
Dengler, Marcus, Dr.	Phys. Oc., CTD / Microstructure	GEOMAR
Domeyer, Bettina	Porewater Geochemistry	GEOMAR
Dullo, W-Christian, Prof. Dr.	Mini-Lander / CTD	GEOMAR
Gasser, Beat, Dr.	In situ pumps	IAEL
Gier, Jessica	Microbiology	GEOMAR
Glud, Anni	Profiler, Microsensors	SDU
Johnston J.C. Ernesto	Foraminiferal Ecology	IMARPE
Koy, Uwe	Technician Physical Oceanography	GEOMAR
Krahmann, Gerd, Dr.	Phys. Oc., Glider / CTD	GEOMAR
Kriwanek, Sonja	Technician Benthic Fluxes	GEOMAR
Larsen, Morten, Dr.	Profiler, Microprofiling	SDU
Lomnitz, Ulrike	P-Geochemistry	GEOMAR
Nitschkowsky, Dörte	Fe-Geochemistry	GEOMAR
Petersen, Asmus	Technician, Lander/Coring	GEOMAR
Reichert, Patrick	Tracer Geochemistry	GEOMAR
Salazar, Jorge A.C.	Foraminifera Ecology	IMARPE
Schüßler, Gabriele	Technician, Microbiology	GEOMAR
Schweers, Johanna	Microbiology	GEOMAR
Steigenberger, Sebastian	Fe-Geochemistry	GEOMAR
Stolpovsky, Konstantin	Video, Benthic Modelling	GEOMAR
Surberg, Regina	Technician, Porewater Geochem.	GEOMAR
Thoenissen, Verena	Porewater Geochemistry	GEOMAR
Treude, Tina, Prof. Dr.	Microbiology	GEOMAR
Trinkler, Sven	Geochemistry	GEOMAR

At the 5th Jan. the scientific team was joined by French (LEGOS) and Peruvian (IMARPE) scientists as well as Dr. E. Breitbarth (GEOMAR), who provided support to establish the trace metal laboratory.

GEOMAR, Helmholtz-Zentrum für Ozeanforschung Kiel Wischhofstr. 1-3 24148 Kiel / Germany Internet: www.geomar.de**,** e-mail: ssommer@geomar.de

IAEA International Atomic Energy Agency, Monaco, e-mail: b.gasser@iaea.org

IMARPE, Instituto del Mar Peru Esquina Gamarra y General Valle s/n Chucuito – Calloa / Peru Internet: www.imarpe.pe e-mail: mgraco@gmail.com

LEGOS Institut de Recherche pour le Développement Research Unit "LEGOS" UMR 5566 (CNES/CNRS/IRD/UPS) 18 avenue Edourd Belin**,** 31401 Toulouse Cedex 9 / France Internet: www.legos.obs-mip.fr e-mail: aurelien.paulmier@legos.obs-mip.fr

SDU University of Southern Denmark, Institute of Biology, Campusvej 55, 5230 Odense, e-mail: aglud@biology.sdu.dk,

UMass School of Marine Sciences and Technology University of Massachusetts, Dartmouth 706 Rodney French Blvd New Bedford, MA 02744-1221 / USA Internet: www.umassd.edu**,** e-mail: maltabet@umassd.edu

3 Research Programme

Oxygen Minimum Zones are key regions for the biogeochemical cycling of major elements. Questions arise of how OMZ´s are maintained and what are the potential feedbacks of benthic nutrient release on presently observed spreading of OMZ´s. The research cruise to the Peruvian OMZ was conducted within the context of the 2nd phase of the Kiel SFB-754. Main aims were:

a. to determine the major benthic nitrogen source (N-fixation), sink (denitrification, anammox) and recycling (dissimilatory nitrite reduction to ammonium, DNRA) processes and their quantitative contribution to the total nitrogen turnover at different sites across the Peruvian margin. Particular aspects are the following: (i) to conduct in situ N-flux measurements across the margin in correlation to depth regions characterized with different sedimentary C_{org} contents, and the availability of O_2 and other electron acceptors; (ii) to quantify benthic microbial nitrogen fixation in surface sediments and to identify/quantify the processes linked to it (e.g., iron/manganese reduction, sulfate reduction, sulfide oxidation); (iii) to quantify denitrification mediated by foraminifera; (iv), resolve triggers controlling the NO_3^-/NO_2^- partitioning between DNRA and denitrification, and (v) to determine benthic nitrogen fractionation.

b. to quantify carbon degradation as well as redox-sensitive iron, phosphate and silicate release rates in situ

c. to carry out a physical-biogeochemical measurement program to improve the understanding of the benthic contribution to the nutrient budget in the Peruvian OMZ. Our primary objectives are to: i) quantify diapycnal fluxes of nutrients (NH_4^+, P, Fe, and Si) from the sediments across the benthic boundary into the stratified interior ocean using microstructure profiling (shipboard operated measurements and autonomous measurements by a Microrider system mounted on a Glider) in combination with time series of currents and physical parameters recorded by moorings and water sample profiles of solutes; ii) investigate pathways and transport of solutes within the benthic boundary layer (BBL) and the stratified water column by measuring the distribution of radium isotopes (223Ra, 224Ra, 226Ra, 228Ra) in combination with solute concentrations and velocity time series from current profiler mounted to landers that will be deployed along the continental slope and the shelf; iii) quantify the effect of bottom currents and turbulence on the benthic turnover and release and uptake of solutes. These measurements will

further allow a detailed investigation of mixing processes in the benthic boundary layer and the lower stratified layer of the water column.

In order to approach these objectives hydrographical measurements were conducted closely linked to geochemical measurements in the water column as well as in the sediment. The focus of the investigations was on a depth transect at 12° S (Figs. 3.1 and 3.2). This site was also part of the research programme of the Meteor cruises M90, M91, and M93. Along this depth transect six stations at water depths of about 70, 150, 250, 400, 750, and 1000 m were designated as main sites for which a coherent data set of all physical, biogeochemical and microbiological measurements from the different working groups will become available (Fig. 3.2). In addition some parameters such as porewater geochemistry or benthic flux measurements were conducted at a higher spatial resolution (Fig. 3.2). Time series measurements of currents and physical properties of the water column were conducted using 5 different moorings in addition to 4 benthic mini-landers that were equipped with upward-looking ADCP´s and a Glider swarm (Fig. 3.2). The instruments were deployed until the end of Meteor cruise M93. Measurements of the microstructure and turbulent mixing of the water column were conducted using a shipboard operated microstructure CTD. Water sampling for nutrients, nitrogen isotopic and N_2/Ar analyses, Fe and particles were based on CTD water sampling rosette casts. The measurements in the water column were supplemented with deployments of in situ pumps and GoFlow casts. In situ pumps were used for radiotracer measurements as well as for the determination of the C/N/P elemental composition of suspended particles. GoFlow casts were conducted to investigate Fe geochemistry of the water column. The benthic program includes in situ flux measurements using benthic landers equipped with 2 chambers (BIGO, Biogeochemical Observatory) as well as a transecting micro-sensor profiling lander. Sediment samples for geochemical and microbiological measurements were taken using a TV-guided multiple corer (MUC) and a gravity corer (GC). Sediments recovered from the BIGO flux chambers were also used for these analyses. Further sediment samples were taken using the MUC for ex situ laboratory incubations to determine processes involved in the nitrogen cycle as well as for foraminifera ecological investigations. From selected stations samples of vacuolated sulphide-oxidizing bacteria were taken to study their role in the turnover of nitrogen species as well as the transient storage and release of phosphorous.

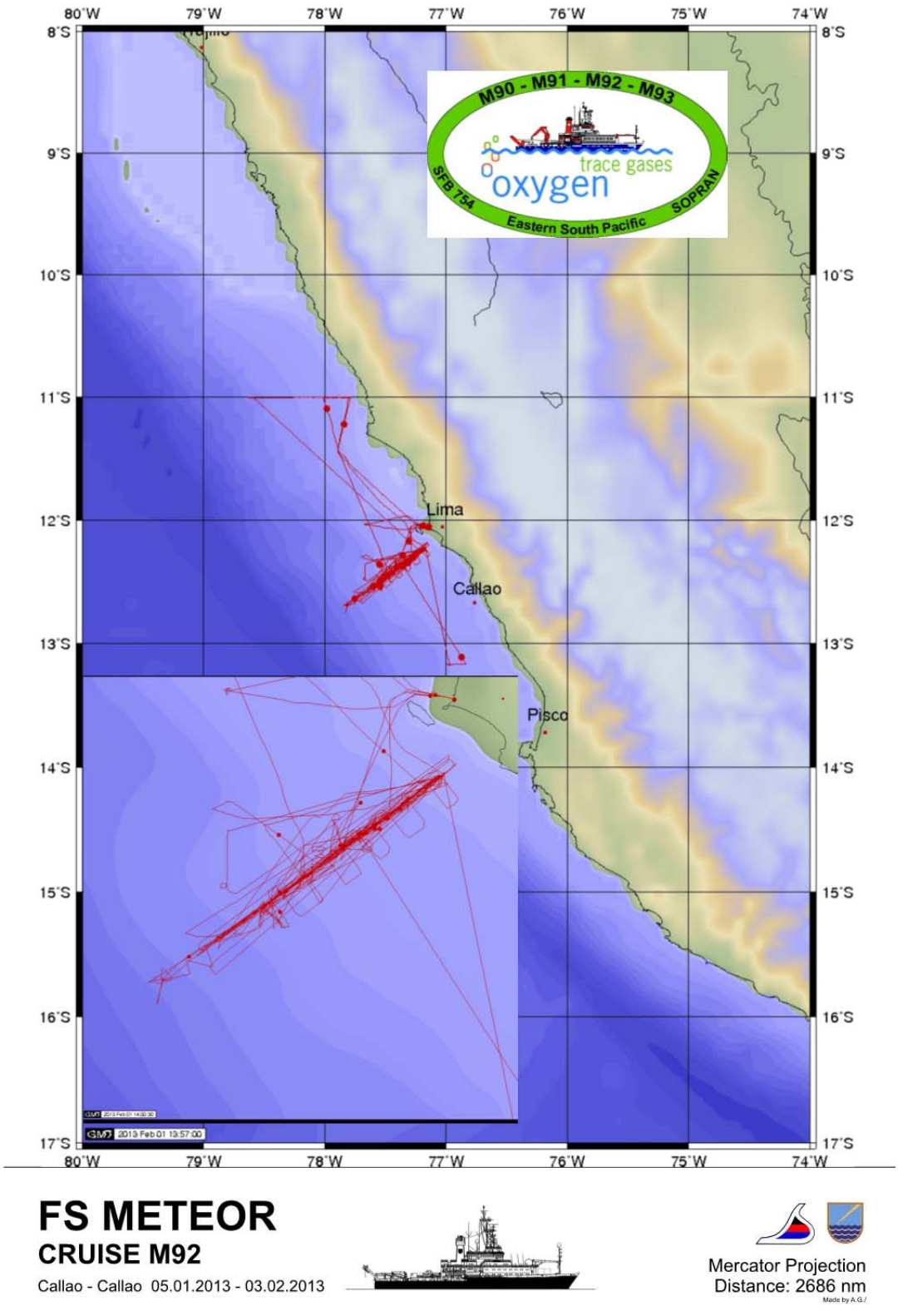

Fig. 3.1 Track chart and sites investigated during of R/V METEOR Cruise M92 showing the 3 different working areas at 12°S, 13°S and 11°S. Major focus was on the depth transect at 12°S.

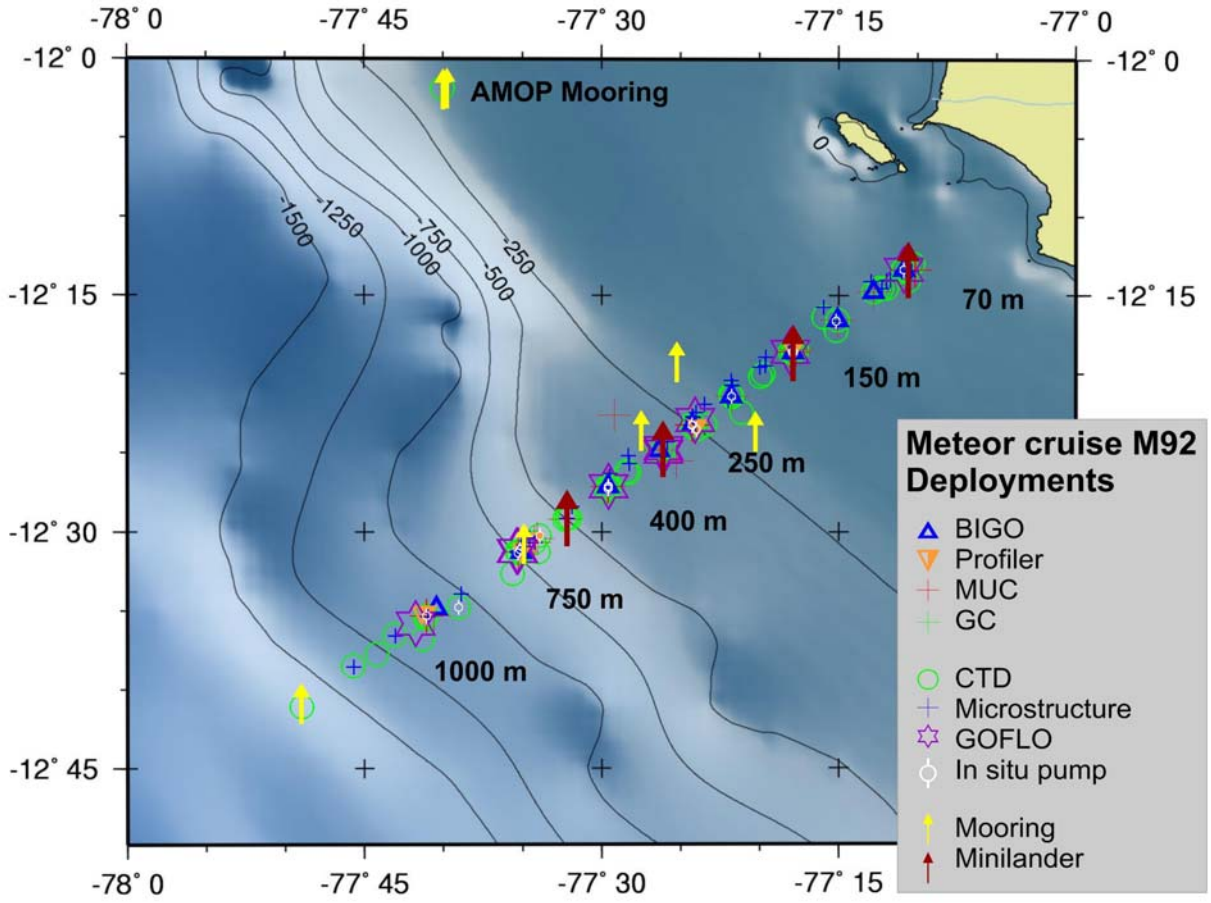

Fig. 3.2 Detailed station map of the 12°S working area. The entire depth transect covers water depths of 70 to 1500 m and a horizontal distance of about 45 nm. The deployment of the AMOP mooring was conducted within a French-Peruvian-German collaboration as part of the AMOP project (Activity of research dedicated to the Minimum of Oxygen in the Eastern Pacific).

Lastly, intense bathymetrical mapping (65h) was conducted in the 12° S working area. Knowledge about the bathymetry is important for the calculation of locations where the energy of incident internal waves is dissipated. This affects exchange of solutes across the benthic boundary (Schafstall et al. 2010) as well as the particle sorting and consequently benthic biogeochemistry and ecology (e.g. Mosch et al. 2012).

4 Narrative of the Cruise

On the 2nd of January a small group of scientists arrived in Callao on Meteor ahead of the main group in order to unpack the containers and to install the instruments on board of the RV Meteor. Participants from LEGOS (France) and IMARPE (Peru) institutions had already boarded RV Meteor prior to January 2nd to prepare the long-term mooring AMOP. On 5 Jan. RV Meteor left Callao harbour in order to deploy the AMOP mooring at a station nearby Callao in a water depth of about 180 m. After successful deployment the RV Meteor went back to Callao to disembark the French and Peruvian technicians.

In the morning of the 6 Jan. RV Meteor left Callao to head towards the main working area at 12° S. This depth-transect covers water depths from about 70 m to 1500 m and spans over a horizontal distance of about 45 nm. The station work started with deployments of CTD/water sampling rosette and the TV guided multiple corer in order to test the suitability of the ground for further extended biogeochemical measurements also using the BIGO and the Profiler lander. Subsequently, six sites in water depths of about 70, 150, 250, 400, 750, and 1000 m were designated as main sites for which all physical and biogeochemical measurements will become available. During the night work was continued with bathymetrical mapping. Knowledge on bathymetry is very important to assess where the energy of incident internal waves is dissipated which is hypothesized to affect exchange of solutes between the seafloor and the bottom water. In the following days the working programme was continued at the 12°S depth transect with the deployment of Gliders and moorings for hydrographical measurements. In addition 4 mini-landers for current and oxygen measurements were anchored at the seafloor. The glider, moorings and the mini-landers were deployed until the end of the subsequent M93 cruise.

Until the 27 Jan. work at 12°S was continued with the deployment of different gears. The day-programme was dominated by the deployment of CTD casts, in situ pumps, GOFLO, TV-MUC, BIGO-lander and Profiler lander as well as moorings and gliders. During the night alternating deployments of CTD and microstructure CTD were conducted.

On the 27 Jan. the coax-cable for the deployment of video-guided instruments was changed for operations with the gravity corer. On the 28 Jan. we changed our working area to 11°S, which was intensively investigated during cruise M77, for further gravity corer-, microstructure CTD- and CTD deployments. During the night of the 29 Jan. RV Meteor headed back to the working area at 12°S in order to complete gravity corer deployments. On the 30 Jan. we changed our working area to a site at 13°S in order to conduct a deployment of in situ pumps, multiple corer and CTD water sampling rosette. On the 31 Jan. we stopped our scientific working programme due to an unfortunate accident of the electronic engineer who needed to be immediately transferred into the hospital. During all days the weather was calm allowing for smooth and successful operations off the different gears.

5 Preliminary Results

5.1 Bathymetry and sea floor imaging

S. Sommer, M. Dengler, T. Treude

Bathymetrical mapping was conducted to assess the interaction of incident internal waves with the sea floor, which has consequences on particle sorting, benthic exchange processes and mixing in the benthic boundary layer (Schafstall et al. 2010, see also section 5.2.3 Turbulence Measurements) and consequently on the benthic ecology (Mosch et al. 2012). The energy conversion from barotropic and low-mode baroclinic tides to high-baroclinic tides of short vertical wave length at the continental slope is controlled by the relative angle of the slope of topography (α) and the angle of propagation of the low-mode baroclinic tide $s^2=(\sigma^2-f^2)/(N^2-s^2)$, where s is the frequency of the internal tide, f is Coriolis parameter and N^2 is stratification.

Topographic slopes are classified as supercritical, critical or subcritical when they are greater than, equal to or less than the internal wave slope, respectively (e.g. Holloway 1985). Upon reflection, internal waves preserve their angle to the horizontal rather than to the reflecting surface (Phillips, 1977), so that reflection from slopes near the critical angle leads to greater shear stress and the development of turbulence at the bottom boundary generating a bottom nepheloid layer with associated turbid plumes (Cacchione and Drake, 1986; Garrett and Gilbert, 1988). Under transmissive conditions, the energy of internal waves is transferred upslope, thereby bottom water velocities accelerate and bottom shear stress intensifies. Such conditions can impede settlement of fine-grained material and lead to the development of bottom nepheloid layers, controlling the deposition of sediment in shallow water depth (Cacchione and Drake, 1986). Under supercritical conditions internal wave energy is reflected back into the ocean. Internal waves are often the dominant factor for mixing at the continental boundary, in particular close to the bottom boundary layer.

A total of 65.7 h of bathymetrical mapping was conducted using the EM122 shipboard system covering a distance of 458.4 nm mainly to map the 12°S area (see station list). Prior to the deployments of the moorings the respective sites were mapped as well.

In order to get a visual impression of the surface sediments all multiple corer deployments were conducted video-controlled. Seafloor images revealed that the sediments from the shallowest station at 73 m water depth down to about 300 m were densely covered with sulphur oxidizing bacterial mats, Fig. 5.1.1. This observation is similar to observations that were made during Meteor cruise M77-1 (Mosch et al. 2012). At 410 m water depth no sulphur bacteria were visible on the sediment surface. Instead exposed foraminiferal sands became apparent. Foraminiferal sands were further observed at a water depth of 648 m. At depths of 505 m the seafloor was hard-ground and did not allow for sampling. In greater water depths at 750 m the sediment was bioturbated and colonized with epibenthic organisms.

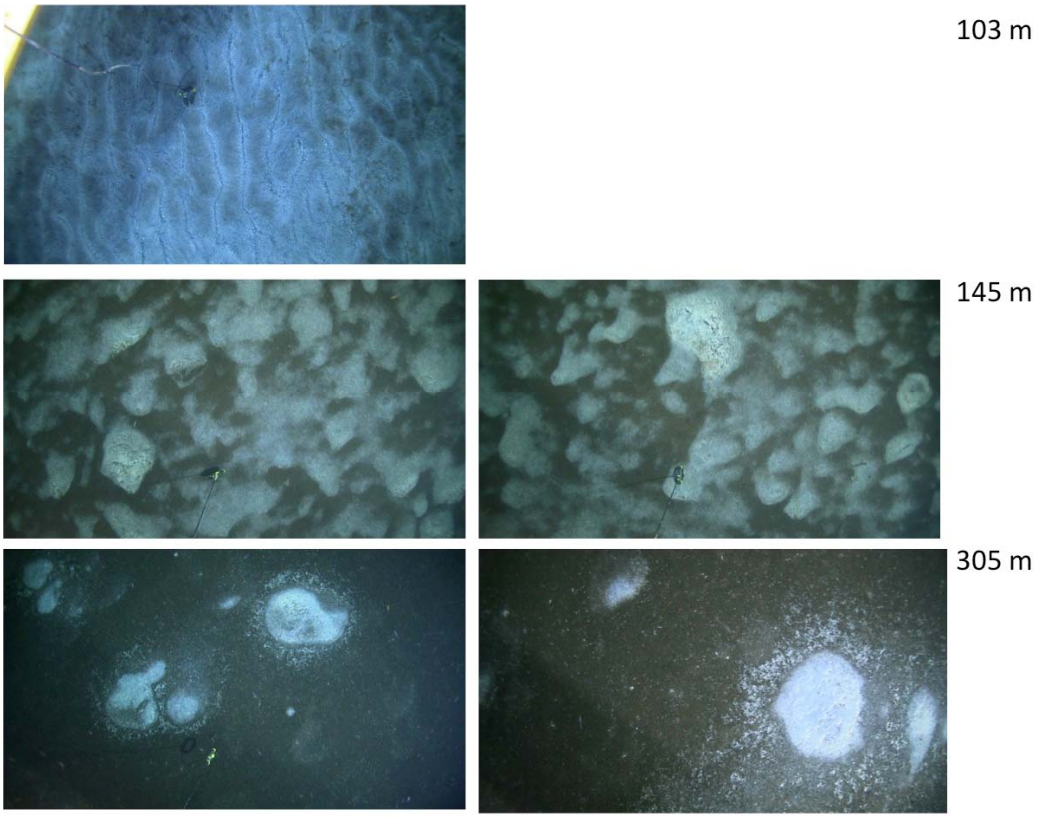

Fig. 5.1.1 Surface sediments covered with sulphur oxidizing bacterial mats. Photos were taken during video controlled deployments of the multiple corer (MUC). A weight was attached to the MUC to control the distance of the gear to the sediment surface.

5.2.1. Glider, Moorings, Mini Lander

G. Krahmann, M. Dengler, C. Dullo, U. Koy

Glider deployments

During M92 seven autonomous glider systems manufactured by Teledyne Webb Research were deployed. Two glider systems (ifm03 and ifm10) were equipped with an external microstructure probe manufactured by Rockland Scientific. These and the other glider systems (ifm06, ifm07, ifm08, ifm11, and ifm12) were equipped with similar sets of sensors. They encompassed a CTD, an Aanderaa optode to measure dissolved oxygen, and a Wetlabs combined CHL-a fluorescence and turbidity sensor. In addition to the regular set of sensors, the Wetlabs sensors on gliders ifm03, ifm07, ifm10, ifm12 included a fluorescence sensor pair to determine the concentration of colored or fluorescent dissolved organic matter (CDOM or FDOM). Because of the elevated power consumption by the microrider it was from the beginning planned to recover ifm03 and ifm10, swap the batteries, and redeploy the gliders. The other five gliders were configured in a regular configuration with enough battery power to run about 7 weeks. All gliders were expected to be recovered on the subsequent leg.

The detailed timing and location of the glider deployments and recoveries is listed in the station list.

During M92 the glider systems worked fine. During the recovery and redeployment of ifm10 it was discovered that the flash card in this glider's microstructure probe had failed after about 4 days. This card was exchanged for one from the UVP system.

On the subsequent leg all gliders but ifm10 were successfully recovered and delivered good data for the full deployment. The otherwise regular satellite telephone contact to ifm10 suddenly ceased on February 7, 2013 after 18:30 UTC. Since the glider at this time was near the entry to the port of Callao/Peru and no other problems had occurred, we presume that the glider was involved in a collision with another vessel.

Mooring deployments

The major aim of the mooring programme carried out during M92 was to investigate the variability of the circulation along the continental slope off Peru, with a focus on meso and sub-meso scale variability. Altogether, 6 water-column moorings were deployed during M92. Five moorings from GEOMAR were deployed in a line perpendicular to the isobaths along the continental slope between 12°S and 13°S (Fig. 5.2.2.1, Table 5.2.2.1). On 4 of these moorings acoustic Doppler current profiler were attached to record upper-ocean velocity time series from the 150m to 300m depth to the surface. Additionally, a moored profiler measuring hydrography, oxygen and velocity while autonomously profiling the water column was deployed on the shelf break at 200m depth. All moorings were successfully deployed at their target positions and depth, despite the fact that deployments needed to be conducted over the starboard side because of limited deck space. The GEOMAR moorings were retrieved during the follow-up cruise M93.

During the first day of the cruise, the AMOP mooring which is jointly funded by France (L'Institut de recherche pour le développement, IRD) and Peru (Instituto del Mar del Peru, IMARPE) was deployed at 12°S, 77.66°W (Fig. 5.2.2.1). The deployment of this mooring was supported by 5 scientists and technicians from IRD and IMARPE that boarded Meteor for this first day of cruise M92 only.

Table 5.2.1.1: GEOMAR Mooring operations during cruise M92.

MMP mooring deployment Peruvian continental slope 77W 12N				**KPO_1099**
MMP (McLane moored profiler)				
Vessel:	Meteor			
Deployed:	14 Jan.	2013	20:25	
Vessel:	Meteor cruise M93			
Recovered:	1 May	2013	16:00	
Latitude:	12°	23.10' S		
Longitude:	077°	19.99' W		
Water depth:	198			
Mag Var:	-0.717			
ID	**Depth**	**Instr. Type**	**s/n**	**Notes:**
		Iridium Watchdog	34013908330	worked?
KPO_1099_01	15	M-CTD	12255	worked to Feb. 9th (1200 profiles)
	193	Release AR661	095	Code:
	193	Release AR661	220	Code:

Double ADCP Mooring deployment Peruvian continental slope 77W 12N				**KPO_1100**
Vessel:	Meteor cruise M92			
Deployed:	7 Jan.	2013	20:05	
Vessel:	Meteor cruise M93			

Recovered:	1 May	2013	17:00	
Latitude:	12°	19.338’ S		
Longitude:	077°	25.199’ W		
Water depth:	197			
Mag Var:	-0.683			
ID	**Depth**	**Instr. Type**	**s/n**	**Notes:**
KPO_1100_01	173	ADCP 300kHz up	1962	full record, gaps at mid-depth
KPO_1100_02	173	ADCP 1200kHz down	7279	full record
	195	Release AR861	188	Code:
	195	Release AR661	839	Code:

ADCP Mooring 1 deployment Peruvian continental slope 77W 12N **KPO_1101**

Vessel:	Meteor cruise M92			
Deployed:	8 Jan.	2013	18:47	
Vessel:	Meteor cruise M93			
Recovered:	28 Feb.	2013	22:00	
Latitude:	12°	23.665’ S		
Longitude:	077°	27.405’ W		
Water depth:	302			
Mag Var:	-0.633			
ID	**Depth**	**Instr. Type**	**s/n**	**Notes:**
KPO_1101_02	276	Microcat TC	1269	full record
KPO_1101_01	276	ADCP 75kHz LR up	12530	full record, gaps at mid-depth
	300	Release AR861	975	Code:
	300	Release AR661	189	Code:

ADCP Mooring 2 deployment Peruvian continental slope 77W 12N **KPO_1102**

Vessel:	Meteor			
Deployed:	18 Jan.	2013	20:16	
Vessel:	Meteor			
Recovered:	28 Feb.	2013	18:30	
Latitude:	12°	30.820’ S		
Longitude:	077°	34.820’ W		
Water depth:	707			
Mag Var:	-0.500			
ID	**Depth**	**Instr. Type**	**s/n**	**Notes:**
KPO_1102_01	130	Microcat TC	1322	full record
KPO_1102_02	130	ADCP 300kHz up	2379	full record
	451	Release AR661	635	Code:
	451	Release AR661	659	Code:

ADCP Mooring 3 deployment Peruvian continental slope 77W 12N **KPO_1103**

Vessel:	Meteor cruise M92			
Deployed:	10 Jan.	2013	22:33	
Vessel:	Meteor cruise M93			
Recovered:	28 Feb.	2013	15:30	
Latitude[1]:	12°	41.015’ S		
Longitude[1]:	077°	48.848’ W		
Water depth:	1705			
Mag Var:	-0.500			
ID	**Depth**	**Instr. Type**	**s/n**	**Notes:**
KPO_1103_01	328	Microcat TC	0952	full record
KPO_1103_02	328	ADCP 75kHz up	2379	full record
KPO_1103_03	407	RCM-8	9344	full record
KPO_1103_04	703	RCM-8	12004	full record
	1703	Release AR861	271	Code:
	1703	Release AR661	121	Code:

[1] Position considers back-spacing of the mooring after anchor release.

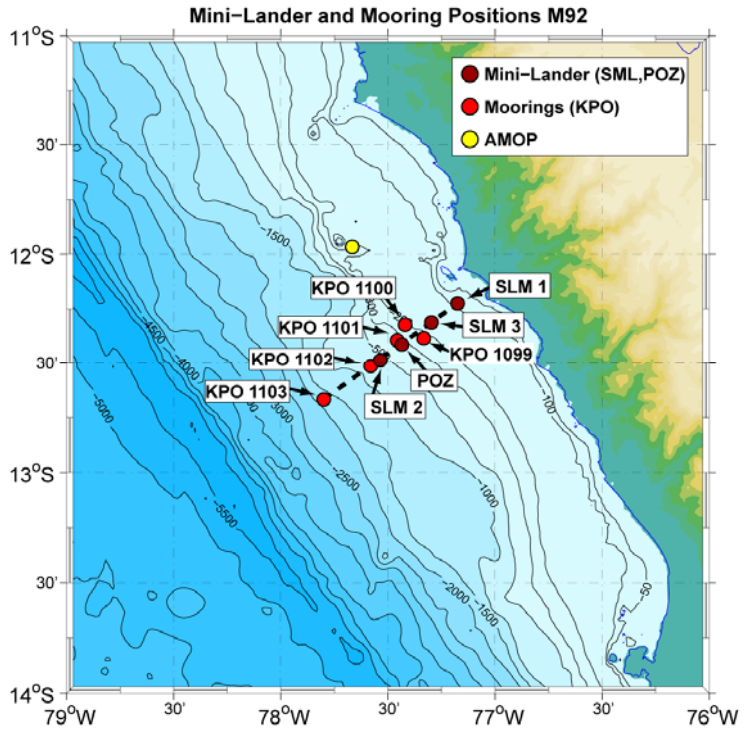

Fig. 5.2.1.1 Positions of moorings and Mini-Landers deployed during cruise M92 and bathymetry (contours).

Satellite Mini Lander

In order to study the spatial and temporal variability of the water mass dynamics, the mooring array (Fig. 5.2.1.1) was completed by the deployment of three identically equipped small sized lander systems (SLM 1, SLM 2, SLM 3) and one prototype lander (POZ) (Fig. 5.2.1.2a).

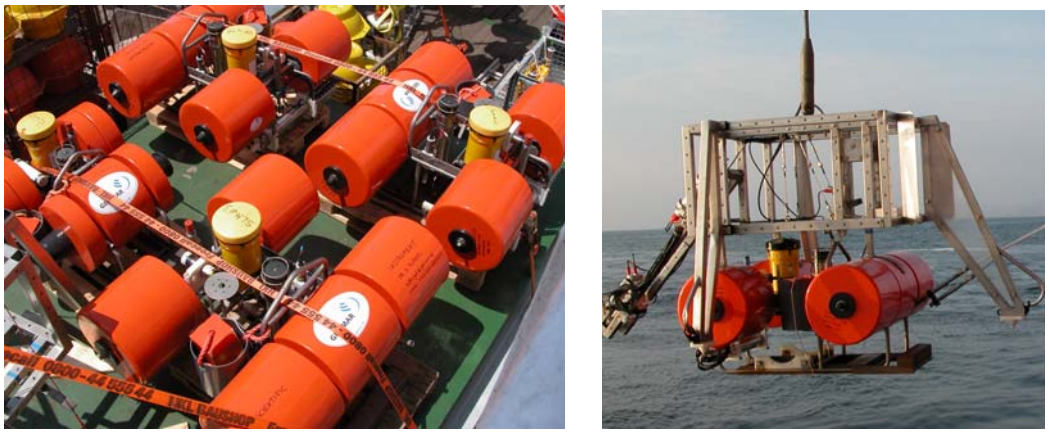

Fig. 5.2.1.2 **a.** small sized landers on deck of RV Meteor **b.** SLM2 mounted below the video guided launcher.

These lander systems recorded every five minutes bottom water dynamics during the full length of the deployment time of max. 51 days. The landers were deployed using by a video guided launcher (Fig. 5.2.1.2b). For precise position see Table 5.2.1.2.

Table 5.2.1.2 Position of the Mini lander deployments along the 12° depth transect across the Peruvian continental slope.

Lander:	Deployment:	UTC:	Lat:	Long:	Depth:	Recovery:
SLM2	09.01.2013	14:34	12°29.22' S	077°32.12' W	498 m	28.02.; 09:13
POZ	09.01.2013	16:24	12°24.84' S	077°26.08' W	299 m	01.03.; 14:25
SLM 1	11.01.2013	23:06	12°13.51' S	077°10.50' W	073 m	01.03.; 19:14
SLM 3	12.01.2013	22:55	12°18.73' S	077°17.81' W	145 m	01.03.; 16:45

The POZ-lander system is equipped with a RBR XR-420CTm Conductivity-Temperature-Depth (CTD) profiler, a high precision Paroscientific Intelligent pressure sensor with an accuracy of 0.015%, and an oxygen optode (3830). The system also comprises a RDI Workhorse Sentinel 300 ADCP. In addition, the lander has a K/MT 562 releaser from K.U.M. Umwelt- und Meerestechnik GmbH, Kiel to drop the anchor weight before recovery. A Novatech beacon and flasher operates after the lander returned to the sea surface in order to locate its position. The SLM landers (1-3) have exactly the same instrumentation, however, they carry additionally a RBR fluorometer, an optical turbidity logger, and a SBE 43 pH sensor. Prior to the deployment, all pH sensors were calibrated on board with solutions of different but exactly determined pH values. The oxygen optodes were calibrated on board as well applying normal seawater and de-oxygenated seawater of known concentrations determined by the Winkler method. Each measurement was replicated 4 times.

5.2.2. Physical water column structure / CTD measurements, CTD calibration

G. Krahmann, M. Dengler, C. Dullo

A total of 84 CTD-profiles were collected. During the whole cruise the GEOMAR SBE#3 with a Seabird SBE 9 CTD rosette system was used. The CTD system was equipped with one Digiquartz pressure sensor (s/n 61184) and double sensor packages (temperature 1 = s/n 4673, temperature 2 = s/n 2814, conductivity 1 = s/n 3366, conductivity 2 = s/n 2512, oxygen 1 (sbe 43) = s/n 1314, oxygen 2 (sbe 43) = s/n 0194).
Data acquisition was done using Seabird Seasave software version 7.21k. The CTD was mounted on the GO4 rosette frame with a 24 bottle rosette sampling system with 10 l bottles. In varying configurations a maximum of 21 bottles were attached to the rosette.
The GEOMAR Guildline Autosal salinometer #8 was used for CTD conductivity cell calibration (operated by G.Krahmann). Calibration during operation was done in two ways: IAPSO Standard Seawater (P150, K15=0.99978) was measured at the beginning of the salinometer use. In addition, a so called “substandard” (essentially a large volume of water with constant but unknown salinity), obtained from deep bottles from the CTD casts was used to track the stability of the system.
The conductivity calibration of the downcast data was performed using a linear fit with respect to conductivity, temperature, and pressure (for all profiles except profile 62 the primary set of sensors was used and calibrated with C_corrected = C_observed -0.012412 - 2.7006e-07 * P -

0.00044235 * T +0.0042561 * C; for profile 62 the secondary set of sensors was used with the calibration C_corrected = C_observed 0.031 4 +1.0973e-06 * P +0.0011308 * T -0.011362 * C). Using 67% of the 61 samples for calibration an r.m.s. of 0.00012 S/m corresponding to a salinity of 0.0012 PSU was found for the downcast. We chose the downcast as final dataset as: 1) Sensor hysteresis starts from a well defined point, and 2) the incoming flow is not perturbed by turbulence generated by the CTD-rosette.
The oxygen calibration of the downcast data was similarly done using a linear fit with respect to oxygen concentration, temperature, and pressure (for all profiles except profile 62 the primary set of sensors was used calibrated with O_corrected = O_observed + 0.57287 + 0.0018213 * P + 0.084954 * T -0.020711 * O, for profiles 62 the secondary set of sensors was used with the calibration O_corrected = O_observed 0.81411 + 0.0016715 * P + 0.0035671 * T + 0.011325 * O). Using 67% of the 347 samples r.m.s uncertainties of 0.75291 and 1.048 µmol/kg were determined.
Starting from CTD profile 44 an Underwater Vision Profiler (UVP) manufactured by Hydroptic and on loan from the Observatoire Océanologique de Villefranche-sur-Mer/France was attached to the CTD-Rosette. On all but a few CTD profiles after #44 this system collected images of particles within the water column. Repeated UVP profiles were thus collected along the 12°S section as well as along the zonal 10°S section and at 13°S
Additionally after CTD profile #18 a single 300kHz workhorse ADCP system, manufactured by Teledyne/RDI was attached to the CTD frame. The ADCP was mounted looking downward and was used to observe currents close to the seafloor. To collect reliable velocity data from this depth region, CTD upcasts were interrupted for a period between 3 to 5 minutes at 50m to 70m above the bottom of the ocean.

5.2.3 Turbulence measurements using the microstructure sensor

M. Dengler, C. Dullo, G. Krahmann

An extensive microstructure measurement programme was carried out aiming at quantifying diapycnal fluxes of solutes along the Peruvian margin and identifying the dominant physical processes responsible for elevated mixing in the Peruvian upwelling region. It combined the research objectives of two projects: Subproject A8 of SFB 754 studying solute fluxes and Subproject 11 of the BMBF-Verbundvorhaben SOPRAN which focuses on diapycnal fluxes and subsequent out-gassing of trace gas N_2O. The measurement programme consisted of autonomous microstructure sampling by two gliders equipped with a MicroRider microstructure instrument (Rockland Scientific), and of shipboard microstructure sampling using a profiling system manufactured by Sea & Sun Technology.

Glider-MicroRider package: As mentioned in section 5.2.1 the MicroRiders were attached to the top of gliders ifm3 and ifm10. The glider-MicroRider package allows sampling of autonomous microstructure profiles for periods of up to 4 weeks per deployment without requiring additional ship time except for glider deployment and recovery. Altogether, each package was deployed twice, but only recovered once during M92. The final recovery of ifm3 was conducted during the follow-up cruise M93, while satellite communication to ifm10 ceased on February 7, 2013 after

18:30 UTC. To date, the ifm10 system could not be recovered. Each MicroRider was equipped with two microstructure shear sensors and two fast-responding temperature sensors (FP07). No sensor failure was found after the first recovery and the same set of sensors detailed in table 5.2.3.1 was used during both deployments of each glider.

Table 5.2.3.1 Deployment schedule and configuration of MicroRider/Glider packages.

Glider mission / MR	Date and time (UTC)	Channel and shear sensors, sensitivity and orientation	Channel and Temp. sensors
ifm03-1 MR sn 57	07 January 14:26 – 25 January 18:54	S1: M845, S_0=0.0661, w' (vert.) S2: M844, S_0=0.0601, y'(horiz.)	T1: T606 T2: T604
Ifm10-1 MR sn 66	15 January 15:36 – 25 January 18:00	S1: M774, S_0=0.0786, w' (horiz.) S2: M903, S_0=0.1002, y'(vert.)	T1: T442 T2: not used
ifm03-2 MR sn 57	27 January 17:32 – 28 February 20:00†	S1: M845, S_0=0.0661, w' (vert.) S2: M844, S_0=0.0601, y'(horiz.)	T1: T606 T2: T604

† - Recovered during FS Meteor cruise M93

Microstructure Profiling: The ship-based microstructure measurements were performed using a MSS90-D profiler (MSS: MicroStructure System: S/N 32), a winch and a data interface. The loosely-tethered profiler was optimized to sink at a rate of 0.55 ms^{-1}. In total, 273 profiles were collected during 41 microstructure stations. The profilers were equipped with three shear sensors, a fast-response temperature sensor, and an acceleration sensor, two tilt sensors and conductivity, temperature, depth sensors sampling with a lower response time. In addition, a fast responding oxygen sensor, hand-made by Anni Glud (SDU) was attached to the profiler from profile 66, MSS station 18 (CTD Station 38) onward. All sensors worked well and no sensor except the fast oxygen sensor needed to be replaced. Presumably due to a collision with a particle in the water column, the fast oxygen sensor broke during MSS profile 117. A new fast oxygen sensor was mounted to the probe before MSS profile 166 (MSS station 29) and was used until the end of the cruise. Starting at MSS station 23 (profile 119), bad data was occasionally received by the deck unit. It turned out that the cable connecting the winch with the profiler had a water leakage close to the profiler. The problem was fixed before MSS station 26 (profile 148) by removing 30m of cable at the profiler end. During the whole cruise shear sensor sn 123 was attached to channel S1, shear senor sn 029 was attached to S2 and shear sensor sn 052 was attached to S3.

5.3.1 Water column nutrient and O_2 geochemistry

M. Dengler, R. Surberg, S. Sommer

Benthic flux measurements that were conducted during the M77 cruise (2008) along a latitudinal depth transect at 11°S showed that particularly at the shelf and upper slope high amounts of

NH_4^+, dissolved phosphate (TPO_4), silicate and Fe^{2+} are released into the bottom water (Bohlen et al. 2011, Noffke et al. 2012). To date the fluxes of solutes from the sediment to the stratified water column and their contribution to the total solute budget of the oxygen minimum zone are poorly quantified. In addition transport across the shelf and slope is also hardly determined. Coastal upwelling (e.g. Brink et al. 1983) is considered as major transport mechanism to supply nutrients to the mixed surface layer where they contribute to sustain high primary productivity. Near continental boundaries turbulent mixing provides another mechanism that transports nutrients and other solutes to the sea surface and entrain them into the surface mixed layer. In fact several studies suggest that a significant proportion of the biological production in the surface water is driven by turbulent fluxes of nutrients (e.g. Hales et al. 2009, Rippeth et al. 2009, Schaffstall et al. 2010). The combination of microstructure data (see section 5.2.3) in combination with nutrient profiles allows to calculate diapycnal fluxes of nutrients and to relate them to benthic fluxes. For the upwelling region of Mauretania an average nitrate flux in the region of the continental slope and the shelves of $12x10^{-2}$ µmol m^{-2} s^{-1} was calculated (Schafstall et al. 2010).

During the cruise NO_2^-, NO_3^-, phosphate (PO_4^{2-}) and silicate (SiO_2) were measured on-board using an QuAAtro autoanalyzer (Seal Analytical) with a precision of ±0.1 µmol L^{-1}, ±0.1 µmol L^{-1}, ±0.2 µmol L^{-1}, and ±0.24 µmol L^{-1} respectively. A total of 45 CTD/water sampling rosette casts were sampled for nutrients with major focus on the 12°S transect and to a minor extent on the 11°S transect. For the station data of the different CTD/water sampling rosette casts used for nutrient analyses please see the station list. Those casts, which were used for nutrient analyses are indicated by “Nutrients”.

As an example, the distributions of NO_3^- and NO_2^- in the water column are shown in figures 5.3.1.1 and 5.3.1.2. The availability of both N-species is strongly related to the uptake by the sediments (see section 5.4.2). The N-species are very important for driving benthic denitrification and/ or anammox, which results in the loss of reactive nitrogen from the ecosystem releasing N_2 into the environment. Especially under oxygen deficient bottom water conditions at the shelf and the upper slope where the sediments are covered with sulphur bacteria (see also Fig. 5.1.1) a certain proportion of NO_3^-/NO_2^- might be used for the dissimilatory nitrate reduction to ammonium pathway (DNRA). During DNRA NO_3^-/NO_2^- is recycled into NH_4^+, hence reactive nitrogen is retained in the ecosystem opposing the “self-cleaning” effect of denitrification and anammox.

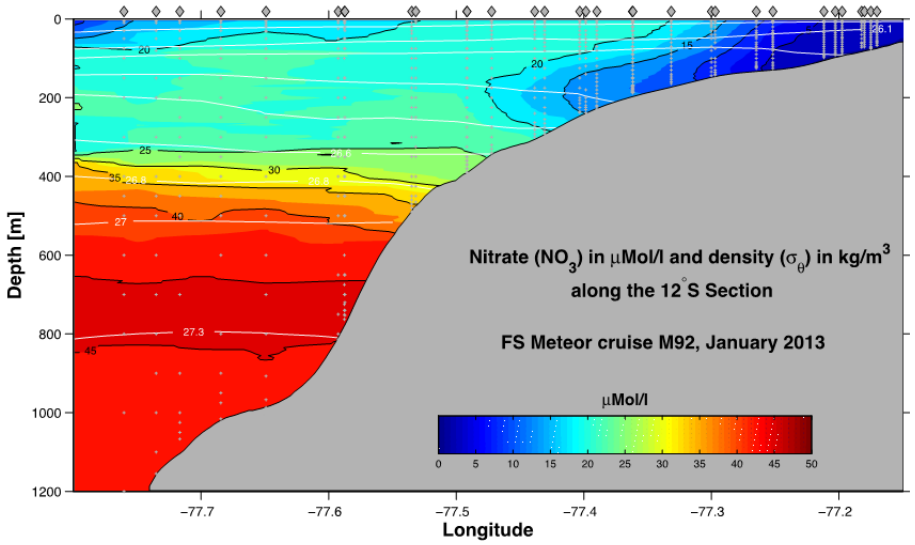

Fig. 5.3.1.1 Nitrate distribution along the depth transect at 12°S. The diamonds and grey dots indicate the position of the CTD casts and the position of sampling respectively.

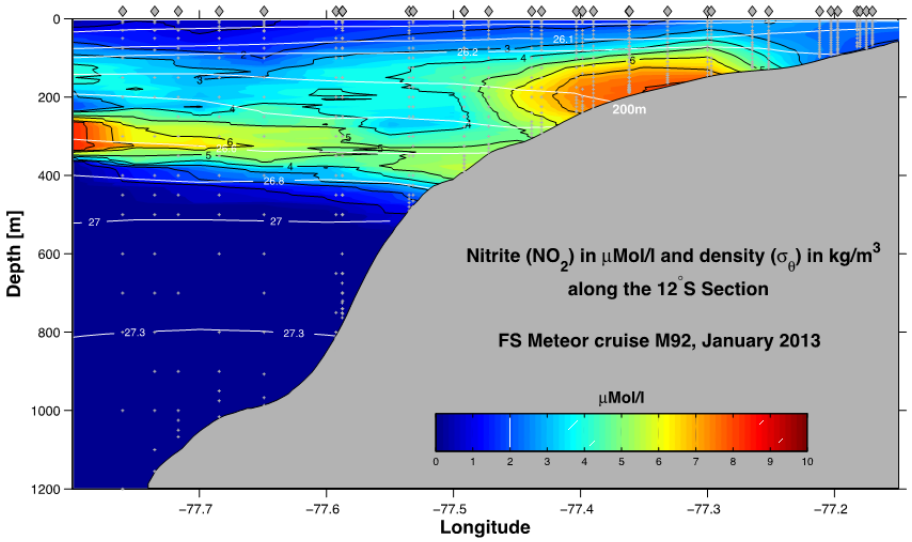

Fig. 5.3.1.2 Nitrite distribution along the depth transect at 12°S. The diamonds and grey dots indicate the position of the CTD casts and the position of sampling respectively.

5.3.2 Water column, nitrogen isotope geochemistry/ N_2/Ar ratios

A. Bourbonnais

Our main goals during the research cruise M92 was to collect samples along hydrographic sections for the analysis of:

a) Dissolved inorganic N (DIN) isotopes: NO_3^- and NO_2^- $\delta^{15}N$ and $\delta^{18}O$, NH_4^+ $\delta^{15}N$ as well as dissolved organic N (DON) $\delta^{15}N$.

b) N_2/Ar and $\delta^{15}N_2$.

c) N_2O $\delta^{15}N$ and $\delta^{18}O$ and $\delta^{15}N$ site preference (in collaboration with Dr. Hermann Bange,

GEOMAR).
d) Near-surface POM $\delta^{15}N$. We also obtained sediment samples from different depths at several stations from the MUC for $\delta^{15}N$ analysis.

Stable isotope measurements represent a useful tool to study N-cycle transformations in marine environments. Both NO_3^- assimilation and denitrification increase the NO_3^- $\delta^{15}N$ (with $\delta=[(R_{sample}/R_{standard})-1] \times 1000$, where R represents the ratio of ^{15}N to ^{14}N) as a consequence of kinetic N-isotope fractionation (e.g. Cline and Kaplan, 1975). An N isotope enrichment factor (ε_{ass} $\varepsilon \approx \delta^{15}N_{substrate} - \delta^{15}N_{product}$) of ~5‰ has been reported for NO_3^- assimilation (Altabet, 2001). The isotope enrichment factor (ε_{den}) associated with microbial denitrification is high, with most recent estimates from both laboratory experiments and natural environments clustering between 20 and 25‰ (e.g. Granger et al., 2008). While N isotopes alone can provide qualitative and semi-quantitative information on single N-cycle transformations, they are less informative in oceanic regions where several N-transformations have overprinting effects on both the NO_3^- concentration and N isotope signatures. However, the measurement of coupled NO_3^- N and O isotope ratios has the potential to disentangle NO_3^- consumption and production processes in environments where they occur simultaneously. This is possible because the $\delta^{15}N$ and $\delta^{18}O$ of NO_3^- are affected in fundamentally different ways during NO_3^- consumption and production (e.g. see Sigman et al., 2005; Bourbonnais et al., 2009).

The unusual inverse fractionation effect for NO_2^- oxidation (Casciotti et al. 2009, $\varepsilon \sim$ -14 to -20‰) represents a potentially powerful approach to help distinguish processes controlling both the NO_3^- $\delta^{18}O$: $\delta^{15}N$ relationship and the production of biogenic N_2. For denitrification, $\delta^{15}NO_2^-$ would be a function of the difference in ε values for NO_3^- and NO_2^- reduction. Since they are similar in magnitude (Bryan et al., 1983), $\delta^{15}NO_2^-$ should be similar to $\delta^{15}NO_3^-$. However if NO_2^- oxidation is a significant fraction of these fluxes, $\delta^{15}NO_2^-$ is lower, as observed in the ETNP consistent with either extensive cycling between NO_3^- and NO_2^- and/or important fluxes to NO_3^- via oxidation of low $\delta^{15}N$ NH_4^+.

The large isotopic and isotopomer signatures associated with N_2O production and consumption yield important source/sink information (Yoshinari et al 1997; McIlvin and Casciotti 2010). In addition to bulk $\delta^{15}N$ and $\delta^{18}O$, the asymmetry of the N_2O molecule permits distinguishing the N isotopic composition of the central (a) and end (b) position N atom (^{15}N site preference (SP) is defined as $\delta^{15}N^{\alpha}$ - $\delta^{15}N^{\beta}$) (Yoshida and Toyoda 2000), which is distinct for N_2O resulting from nitrification or denitrification, and thus potentially allows to differentiate between these different processes.

All samples will be analyzed after the cruise in the laboratory using the following methods:

a) DIN isotope analysis - NO_3^- will be analyzed by Cd reduction to NO_2^- followed by reaction with azide to produce N_2O in sealed septum vials (McIlvin and Altabet 2005) with modifications to prevent over-reduction. When sulfamic acid has been added to remove NO_2^-, no interference occurs from leftover reagent due to maintenance of a high pH until addition of the azide reagent as sulfamic acid reacts with NO_2^- (actually HNO_2) only at low pH. N_2O gas is analyzed using a purge-trap interface (Sigman et al. 2001) to a GV IsoPrime IRMS. Reproducibility is ± 0.2‰ for $\delta^{15}N$ and ± 0.4‰ for $\delta^{18}O$ on sample concentrations as low as 0.5 µmol/kg. Standardization is

against publicly available and certified materials (e.g. USGS32, USGS34, and USGS 35). NO_2^- isotopic composition is measured without prior Cd reduction using a modification of the azide method. These samples are preserved frozen at pH 12 and buffering of the azide reagent is adjusted to bring the pH down to the reaction favorable range of 4 to 5 without O isotope exchange with water. Publically available standards are not yet available but we have exchanged materials with Karen Casciotti's lab. Where $[NH_4^+]$ >0.5 µmol/kg, its $\delta^{15}N$ is measured by hypobromide oxidation to NO_2^- followed by the azide reaction to N_2O (Zhang et al. 2007). Previous removal of NO_2^- by sulfamic acid is equally effective in this case. DON $\delta^{15}N$ can be measured using persulfate oxidation to NO_3^- (Knapp et al. 2005) though these latter analyses will be pursued only on an ancillary, exploratory basis.

b) DG analysis - N_2/Ar and $\delta^{15}N_2$ analyses will be made by pumping, at 5 to 10 ml/min, water samples through a continuous sparger which transfers dissolved gases quantitatively to a continuous flow of the He carrier gas. DG samples require no preparation in the lab and analysis time is about 10 min. Carrier gas is passed through water, CO_2, and software selectable hot-Cu O_2 traps before admittance via an open split to an IRMS. O_2 removal improves the precision of the N_2/Ar and $\delta^{15}N_2$ measurements and eliminates analytical bias associated with changing sample O_2/N_2. Our GV IsoPrime IRMS is fitted with sufficient collectors for simultaneous measurement of N_2 (masses 28 and 29), O_2 (masses 32, 33, and 34), and Ar (mass 40). Gas and isotopic ratios are measured against artificial compressed gas mixtures of N_2, O_2, and Ar close to expected dissolved gas ratios. These reference mixtures are in turn calibrated against compressed air cylinders provided and certified by Dr. Ralf Keeling (SIO). Reproducibility of N_2/Ar and $\delta^{15}N_2$ is better than 0.5‰ and 0.05‰, respectively. Daily calibration is against water equilibrated with air at precisely controlled temperatures of 15.0, 20.0 and 25.0° C. Excess (biogenic) N_2 will be initially calculated against equilibrium values expected from in situ temperature and salinity.

c) N_2O isotopomer analysis - This work will be in collaboration with Dr. Hermann Bange. Analyses will be made directly on samples using a PT-IRMS system, as described above, except for additional time needed for sample gas extraction from the larger volume. Backflushing of the purge-trap system's GC column as recommended by McIlvin and Casciotti (2010) has already been implemented to eliminate interferences in the ^{15}N site preference (SP) determination. Our IRMS has the necessary collector configuration for simultaneous determination of masses 30, 31 (for SP) and 44, 45, and 46 (bulk $\delta^{15}N$ and $\delta^{18}O$). A multiple point calibration of several N_2O gases of known SP (as well as bulk $\delta^{15}N$ and $\delta^{18}O$) will be applied. We plan to exchange reference gases with Karen Casciotti's lab as a first approach to calibrate with subsequent curve fitting and solve for the appropriate parameters.

d) POM and sediment $\delta^{15}N$ analysis - POM and sediment $\delta^{15}N$ will be measured using an elemental analyzer coupled to the IRMS.

Dissolved gas (N_2/Ar) sample analysis will immediately commence for completion within 6 months of collection. In Year 2, DIN and N_2O sample analysis will be the primary activity. We anticipate concluding analytical activity at the end of the second year and start initial data workup and interpretation. In Year 3, results will be written up for publication.

5.3.3 Water column, Fe geochemistry

E. Breitbarth, S. Steigenberger, D. Nitschkowsky

Water and sediment pore water sampling was performed in order to estimate the fluxes and redox chemistry of Fe and its interrelation with P across the benthic-pelagic interface, as well as across the OMZ. The programme of the trace metal group thus consisted of water column sampling for trace metal analyses (dissolved and particulate fraction, measurements of the redox species Fe(II)) and Fe(II) in pore- and bottom water from benthic chambers of the Biogeochemical Observatory (BIGO, see 5.4.2).

Water column sampling for dissolved trace metal analyses was performed using an array of six Teflon coated PVC GoFlo bottles (General Oceanics, Miami, USA) attached to a Kevlar wire that were triggered with manual messengers. Ten stations were sampled, yielding a total of 58 samples (see Tab. 5.3.3.1). After retrieval on deck the water samplers were placed in a holding rack, gently pressurized with N_2 gas (5.0), and the water was 0.22 µm in-line filtered (Millipore, Sterivex) inside a laminar flow bench. Analyses for Fe, Co Ni, Cu, Zn, Cd, and Pb is currently being performed by graphite furnace atomic absorption (ETAAS: Perkin-Elmer Model 4100 ZL) after pre-concentration by simultaneous dithiocarbamate-freon extraction from seawater (Danielsson et al., 1978). Particulate matter was collected on 45 mm 0.22 µm polycarbonate filters using the same set-up and frozen at -20º until analysis via ICPMS after acid digestion.

Table 5.3.3.1 List of stations sampled using GoFlo bottles. Analyzed parameters: dissolved Fe, Co Ni, Cu, Zn, Cd, and Pb concentrations and particulate trace metal concentrations.

	Station number									
	31	60	72	102	112	126	135	190	212	278
Water depth(m)	20	20	20	15	22	20	19	20	20	20
	59	41	32	155	73	170	94	200	37	50
	98	62	43	455	124	420	169	500	54	80
	137	83	55	595	174	620	243	600	71	110
	176	104		645	229	770	314	650	88	140
	215	125		700	298	905	400	700	105	170

In parallel, the CTD casts at stations # 66, 92, 98, 132, 138, 158, 167, 179, 192, 210, 216, and 240 (see station list, section 7) were sampled with full depth resolution for Fe(II) analyses. Fe(II) was analyzed immediately after sampling using chemiluminescent flow injection analyses based on Croot and Laan (2002). For an example of a Fe(II) profile determined at station 158 see figure 5.3.3.1.

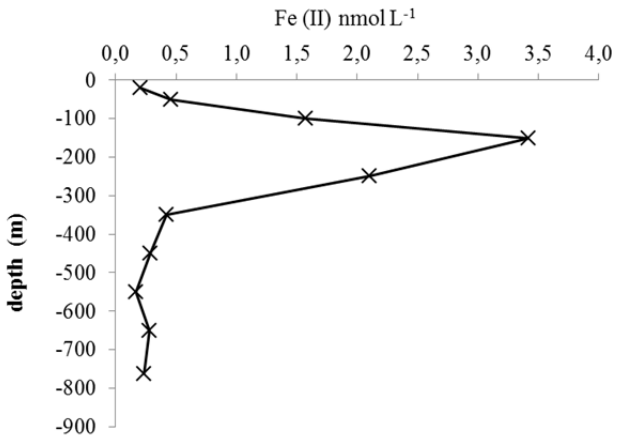

Fig. 5.3.3.1 Example of a Fe(II) profile (station # 158, bottom depth 772 m) clearly showing elevated reduced Fe concentrations in the oxygen deficient water layer.

Nine stations were sampled for Fe(II) concentration analysis from benthic chambers (BIGO, see 5.4.2, station number: 85, 97, 131, 143, 173, 187, 217, 232, 267). For an example of the temporal development of Fe(II) concentrations in benthic chambers see figure 5.3.3.2. In total of 216 Fe(II) samples were analyzed in triplicates directly on board using a spectrophotometric method after ferrozine-Fe(II) complexation based on Koroleff and Kremling (2007) in order to follow Fe speciation during the benthic incubations.

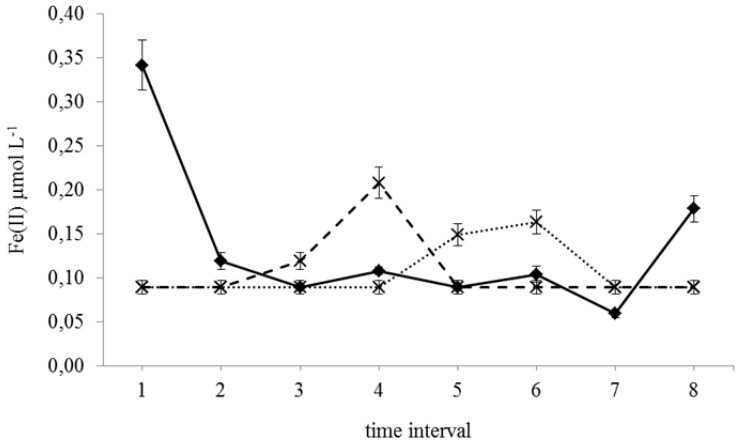

Fig. 5.3.3.2 Development of Fe(II) during the benthic incubation on station # 143, water depth 756m. Legend: Solid line represents bottom water, dashed line Ch1, and dotted line Ch2. Error bars depict standard deviations of three replicate measurements.

5.3.4 Water column, radiotracer geochemistry

P. Reichert, B. Gasser, J. Scholten

The use of radioisotopes as tracers is a very powerful approach for the study of the biogeochemical cycling of major elements between the bottom boundary layer and the stratified water column. Within the present project, radium and thorium isotopes were used to: 1) determine fluxes of solutes of sedimentary origin into the water column, their iso-and diapycnal dispersion and their relative contribution to the total solute budget of the oxygen minimum zone (radium isotopes), and 2) describe the thorium-234, distribution within the sampling zone and use this parameter for the determination of the export of organic carbon out of the euphotic zone.
1) The radium isotopes ^{223}Ra (half-life: 11.4 days), ^{224}Ra (half-life: 3.66 days), ^{226}Ra (half-life: 1600 years) and ^{228}Ra (half-life: 5.75 years) are produced by the decay of thorium radio-isotopes (^{235}U-, ^{232}Th- and ^{238}U-decay series). The radium is released to the water column through sediment pore water. The amount of radium produced in and leaving the sediment is related to the concentration of the parent radionuclides in the sediment. It is possible to use the radium isotopes as tracer for water mixing processes because the behaviour of radium in seawater is conservative so that only diffusive-advective transports and decay, change the radium concentration and distribution in the water column. Information on the radium gradient in the water column allows estimating the time scales of water mixing and the calculation of elemental fluxes from shelf sediments into the bottom boundary layer.
In general the ^{226}Ra concentration in the water column is very homogeneous in the upper first meters and increases with depth, because the main source for this long-lived isotope is the deep-sea sediment. The ^{228}Ra distribution is different, with relatively high concentrations near the sediment and in the surface waters. This distribution is due to the lateral advection of waters, which have been in contact with shelf sediments. In the mid-water depth the concentration of ^{228}Ra is very low because of the short half-life relative to the ocean mixing. The general distributions of ^{223}Ra and ^{224}Ra are roughly the same as the distribution of ^{228}Ra in the water column. A common approach for calculating and quantifying horizontal and vertical mixing processes is the use of models, in which the fluxes are resolved in vertical/horizontal transports and parameterized by constant eddy diffusion coefficients [Ku and Luo, 2008]. These coefficients are determined by fitting model calculations to the radium distribution.
2) ^{234}Th is the first decay product of the natural uranium-238 decay series and shows high reactivity with particles, while its long lived parent ^{238}U has a conservative behavior and remains soluble in seawater. This “scavenging” of ^{234}Th by settling particles causes a separation between daughter and parent nuclide, which makes ^{234}Th a suitable tracer for studying the export of particle associated elements out of the productive ocean surface layer and in particular the export flux of organic carbon (see Rutgers van der Loeff et al., 2006, Buesseler et al., 2006 and references herein). In order to quantify this process, we first determine the flux of ^{234}Th, which is derived from the ratio ^{234}Th to ^{238}U and then multiply it by the ratio C/^{234}Th measured on sinking particles.

During cruise M92, in situ pumps were deployed along a transect at 12°S and at 13°S. Focus was given to the main sites along 12°S at water depths of 70, 150, 250, 400, 750 and 1000 m where all other sampling devices were deployed, which yielded a complete set of parameters for these

sites. In order to take into account the objectives for both the thorium and radium isotope studies, deployment depths were chosen as follows:
For the surface waters and with respect to the ^{234}Th measurements, sampling depths were 5, 10, 20 m, 70 m and 120 m below sea surface at each site, taking into account the chl*a* maximum around 10 m and a secondary one at 70 m depth observed in the CTD profiles acquired just beforehand. For the deeper waters, sampling depths were situated at 50 m steps from the seafloor for the first 3 pumps and at 100 m for the remaining ones, thus respecting a dilution pattern of the concentrations of radium isotopes to be measured.
Each pump was equipped with 2 filters for particles sampling and 2 cartridges for sampling the dissolved ^{234}Th and the radium isotopes. One filter (Nitrex tissue) sampled the >70 µm size class considered to represent the settling particles, and the other filter (micro quartz filter of 1 µm nominal size) sampled the suspended particles. Both radium and dissolved ^{234}Th was sampled by retention on MnO_2 impregnated cartridges (CUNO Micro-Klean III acrylic), the first cartridge being used for quantifying the ^{234}Th concentration and the radium distribution in the water column and the second one for determination of the retention efficiency. For the long-lived isotopes ^{226}Ra and ^{228}Ra we took water samples (1 litre) from the CTD-Rosette at each water depth where we have used the *in-situ* pumps. We also sampled the sediment along the transect at 12°S with the help of a multiple corer by taking pore water samples in different depth intervals of the core to get information about the ^{226}Ra distribution in the sediment core. The upper 10 cm of the sediment core were sampled at 1 cm depth intervals, below every sediment samples in 2 cm intervals.
On board, the Mn-cartridges were washed, partially dried and measured for the short-lived isotopes ^{223}Ra and ^{224}Ra with a RaDeCC system. The RaDeCC system utilizes the difference in decay constants of short-lived Po daughters of ^{219}Rn and ^{220}Rn to identify alpha particles derived from ^{219}Rn or ^{220}Rn decay and hence to determine activities of ^{223}Ra and ^{224}Ra on the Mn-fiber [MOORE, 2008]. The measurement of the ^{234}Th activity will need combustion of the cartridges at the laboratory, where the ash will be analysed by gamma spectrometry. Among the filters of the in-situ pumps, only coarse sized ones were treated on board. Particles from the >70 µm size class were rinsed off the tissue filters and the rinsing water was filtered onto micro quartz filters, which will be analysed back in the laboratory for ^{234}Th beta activity. This non-destructive method enables the subsequent measurement of the carbon content on the same particles, in order to obtain the C/^{234}Th ratio of settling particles. Filters sampling the small sized particles were frozen and will be prepared back at the laboratory for the measurement of the ^{234}Th beta activity.

To summarize, this strategy yielded a total of 7 profiles; 6 profiles were taken along the transect at 12°S and one at 13°S. Depending on the particle load the filtered volume for each sample was expected to vary considerably but sufficient to obtain measurable amounts of radium isotopes. Half of the samples corresponded to more than 1000 L filtered and the other half to 500 1000 L. A visual inspection after deployment of both the coarse and fine sized filters confirmed the high particle load in the samples between 0 and 50 m water depth corresponding to a pronounced chl*a* maximum.

5.4.1 Porewater geochemistry

A. W. Dale, U. Lomintz, V. Thoenissen, B. Domeyer, R. Surberg, S. Trinkler

Objectives

The porewater composition of surface sediments was investigated in order to characterize and quantify sediment diagenetic processes below the oxygen-deficient waters offshore Peru. One aim of this cruise was to further our understanding of the benthic-pelagic coupling in oxygen deficient regions of the ocean by examining key geochemical species whose chemical behaviour and distribution are altered via changes in redox potential. Specific emphasis was placed on the biogeochemical cycling of redox sensitive elements such as N, P and Fe, which are preferentially released from sediments under anoxic conditions. The magnitude of this recycling flux, the relative importance of key control parameters, and the coupling to carbon and sulphur cycles are still poorly understood. In order to overcome this lack of knowledge we performed geochemical analyses of pore water from surface sediments that were retrieved by multiple corer, gravity corer lander deployments.

Methods

Sediment cores were retrieved using the multiple corer (MUC) and the gravity corer in addition to smaller push cores recovered with the BIGO landers. An overview of the sampling stations where porewater was analysed is given in Table 5.4.1.1. After retrieval all cores were transferred to a cooling lab (4°C) and processed within 1-2 hours. Supernatant bottom water of the multicorer-cores was sampled and filtered for subsequent analyses. In general, more than one MUC or BIGO sediment core was taken at the same site, but not necessarily on the same day. For all measurements and sub-samples of redox-sensitive parameters (e.g. Fe, nutrients) the MUC and BIGO cores were sectioned in an argon filled glove at a depth resolution increasing from 0.5 cm at the surface to 2 cm at depth. Porewater was extracted from these sediments using a refrigerated centrifuge at 4000 G for 20 min. Subsequently, the porewater samples were filtered (0.2 µm cellulose-acetate filters) under argon. The sediment remaining in the centrifuge tubes was frozen and shipped back to the onshore laboratory. On several occasions a second core was sectioned without argon at the same depth resolution and porewater extracted by pressure filtration (max. 5 bar) and then filtered (0.2 µm cellulose acetate filters). At each sample depth, sediment samples were also taken for the calculation of sediment density and water content as well as solid phase constituents in the onshore laboratory. These sub-samples were filled into pre-weighed gas-tight plastic vials and stored under argon for subsequent analyses in the home laboratory. Gravity cores were cut lengthwise after recovery and porewater was extracted using Rhizons inserted into the working half of the core with vacuum created by plastic syringes. The first 0.5 ml of pore water extruded through the Rhizons were discarded. Porewater extraction using this method required up to one hour, yielding max. 15 ml of porewater at each depth interval.

A total of 811 porewater samples were recovered and analyzed (Table 5.4.1.1). Porewater analyses of the following parameters were carried out onboard: ferrous iron, nitrate, nitrite, ammonia, phosphate, silicate, alkalinity and hydrogen sulphide. These were measured

photometrically using standard methods described by Grasshoff et al. (1997). Modifications of some methods were necessary for samples with high sulphide concentrations. Samples of the sediment pore water for total alkalinity measurements were analysed by titration of 0.5-1 ml pore water according to Ivanenkov and Lyakhin (1978). Titration was finished until a stable pink colour occurred. During titration the sample was degassed by continuously bubbling nitrogen to remove the generated CO_2 or H_2S. The acid was standardized using an IAPSO seawater solution. The method for hydrogen sulphide determination according to Grasshoff et al. (1997) was adapted for mM pore water concentrations. For reliable and reproducible results, an aliquot of pore water was diluted with appropriate amounts of oxygen-free artificial seawater; the sulphide was fixed by immediate addition of zinc acetate gelatine solution immediately after pore-water recovery. After dilution, the sulphide concentration in the sample was < 50 µmol/l. For the analysis of iron concentrations, sub-samples of 1 ml were taken within the glove bag and immediately complexed with 20 µl of Ferrozin and determined photometrically.

Untreated samples were also frozen for onshore analysis of chloride, bromide, and sulphate by ion-chromatography. Acidified sub-samples (35µl suprapure HCl + 3 ml sample) were prepared for analyses of major ions (K, Li, B, Mg, Ca, Sr, Mn, Br, and I) and trace elements by inductively coupled plasma atomic emission spectroscopy (ICP-AES). DIC, $\delta^{18}O$ and $\delta^{13}C$ of CO_2 will be determined on selected sub-samples in the shore-based laboratories. Finally, in selected cores, filtered porewater samples from the anoxic glove bag were frozen and transported to University of Massachusetts (M. Altabet) for analysis of stable N isotopes (^{15}N, ^{14}N).

Table 5.4.1.1 Stations, porewater sampling method and number of samples measured in multiple corers (MUC), benthic landers (BIGO) and gravity cores (GC).

Station	method	water depth (m)	Lat. [°S]	Long. [°W]	No. samples
6 MUC1	glove bag	142	12°18.540'	77°17.533'	17
17 MUC5	glove bag	253	12°23.329'	77°24.185'	20
17 MUC5	glove bag	253	12°23.329'	77°24.185'	26
26 MUC9	glove bag	305	12°24.894'	77°26.301'	23
30 BIGO2-1	glove bag	306	12°24.905'	77°26.295'	14
36 MUC10	glove bag	145	12°18.708'	77°17.794'	23
55 MUC13	glove bag	70	12°13.496'	77°10.514'	26
56 MUC14	press	70	12°13.492'	77°10.511'	26
57 BIGO1-1	glove bag	142	12°18.712'	77°17.803	11
69 MUC16	glove bag	103	12°14.897'	77°12.704'	27
74 BIGO2-2	glove bag	244	12°23.301'	77°24.284'	14
86 MUC17	glove bag	774	12°31.374'	77°35.183'	22
107 MUC23	glove bag	407	12°27.198'	77°29.497'	20
108 MUC24	press	407	12°27.195'	77°29.493'	23
121 MUC26	press	773	12°31.409'	77°35.195'	23
110 BIGO1-2	glove bag	74	12°13.506'	77°10.793'	12
110 BIGO1-2	press	74	12°13.506'	77°10.793'	8

124 BIGO2-3	glove bag	756	12°31.366'	77°34.997'	12
136 MUC27	press	408	12°27.185'	77°29.508'	8
155 MUC28	glove bag	1025	12°35.377'	77°40.975'	22
159 BIGO1-3	glove bag	989	12°34.911'	77°40.365'	12
163 MUC30	press	1024	12°35.404'	77°41.013'	22
165 BIGO2-4	glove bag	128	12°16.689'	77°14.995'	18
165 BIGO2-4	press	128	12°16.689'	77°14.995'	10
178 MUC33	press	244	12°23.286'	77°24.221'	10
198 MUC34	glove bag	244	12°23.300'	77°24.228'	26
201 BIGO 1-4	glove bag	195	12°21.502'	77°21.712'	19
207 BIGO2-5	glove bag	409	12°27.21'	77°29.52'	12
208 MUC 36	glove bag	296	12°25.59'	77°25.20'	27
208 MUC 36	press	296	12°25.59'	77°25.20'	9
220 MUC39	glove bag	71	12°13.531'	77°10.061'	27
220 MUC39	press	71	12°13.531'	77°10.061'	10
235 MUC42	glove bag	648	12°30.75'	77°34.18'	15
247 MUC45	glove bag	195	12°21.491'	77°21.702'	26
247 MUC45	press	195	12°21.491'	77°21.702'	10
248 MUC46	glove bag	129	12°697'	77°15.001'	26
248 MUC46	press	129	12°697'	77°15.001'	10
249 BIGO1-5	glove bag	101	12°14.90'	77°12.70'	18
254 GC03	Rhizones	407	12°27.192'	77°29.491'	9
255 GC04	Rhizones	188	10°59.99'	78°0.91'	30
263 GC06	Rhizones	361	11°0.00'	78°12.61'	22
265 GC07	Rhizones	1485	10°59.99'	78.38.01'	28
268 GC08	Rhizones	78	12°14.500'	77°9.611'	12
289 MUC50	glove bag	83	10°.59.996'	77°47.398	26

Results (onboard)

A selection of the porewater profiles from sediment cores retrieved during multiple corer deployments are shown in Fig. 5.4.1.1. The data present a clear trend of decreasing accumulation of the products of organic matter degradation such as ammonium and total alkalinity with water depth. For example, on the shelf at 80 m ammonium concentrations at 15 cm sediment depth are 2000 μM, whereas at 1025 m ammonium reaches only 30 μM. These trends are driven by a reduction in the amount and reactivity of reactive organic matter reaching the seafloor with increasing water depth. This trend is further emphasized in the concentration of dissolved silicate which is produced in sediments following the dissolution of biogenic opal. Porewater ammonium concentrations down to 300 m water depth could also be influenced by the sulphide-oxidizing bacteria that inhabit the upper few cm of sediment. These data will be analysed at a later date using numerical reaction-transport models to try and quantify the role of these microorganisms in N cycling at 12 ^{o}S on the Peru margin (e.g. Bohlen et al., 2011). Phosphate and iron concentrations show more complex patterns that will require analyses of solid phases in the onshore laboratory to be interpreted properly.

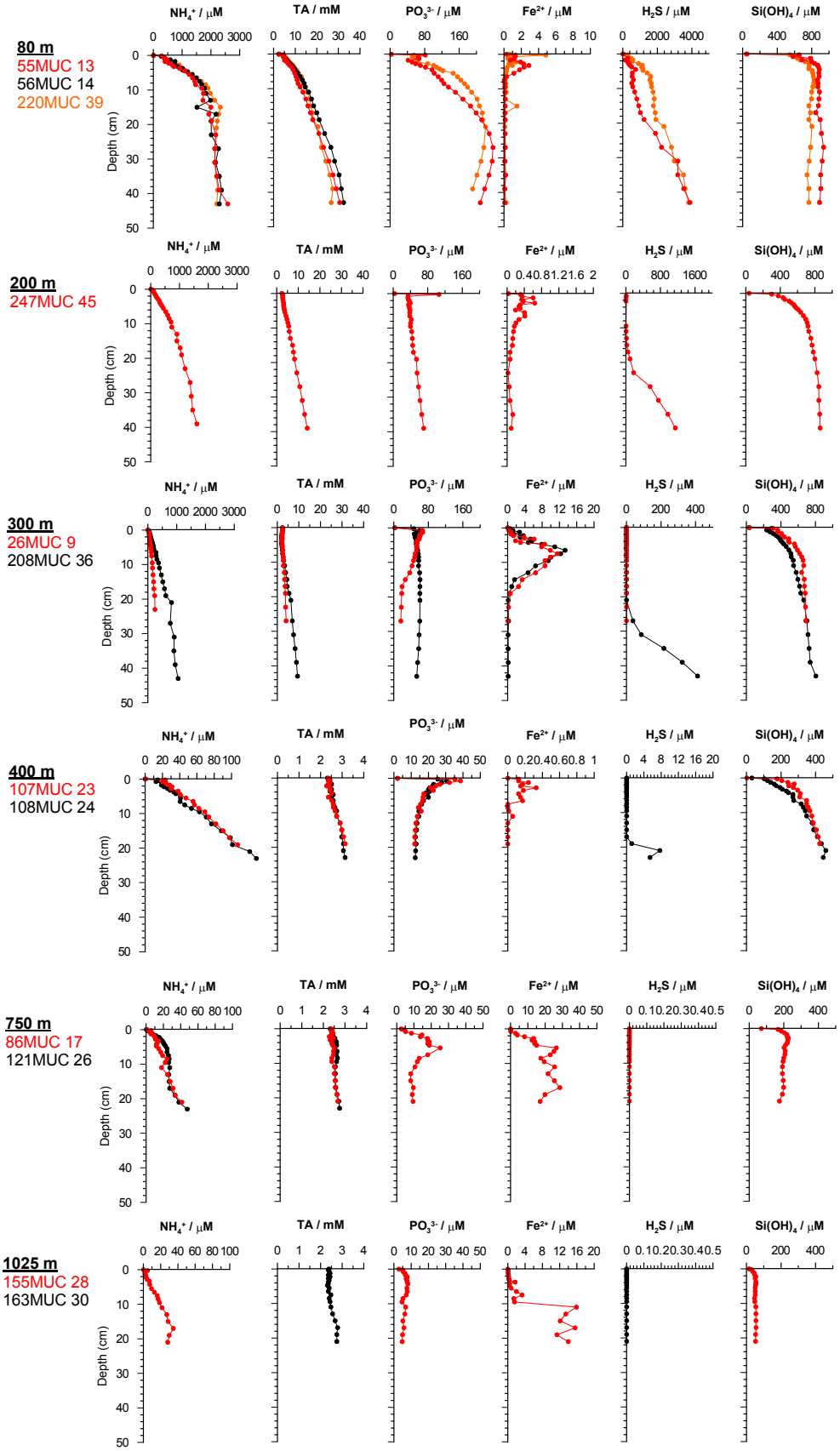

Fig. 5.4.1.1 Measured (symbols) concentration profiles of dissolved ammonium, total alkalinity, dissolved phosphate, ferrous iron, hydrogen sulfide and silicate in sediments sampled by the multiple corer arranged by increasing water depth.

5.4.2 In situ benthic fluxes, BIGO-I and BIGO-II

S. Sommer, A. Dale, S. Kriwanek, S. Cherednichenko

Major task was to determine in situ fluxes of nitrogen species (N_2, NO_3^-, NO_2^-, NH_4^+) as well as P and Fe across the sediment water interface under conditions of different bottom water O_2, NO_3^-, NO_2^- concentrations and C_{org} content of the surface sediments. Total fluxes of the above mentioned parameters were measured in benthic chambers using the Biogeochemical Observatory (BIGO). Two structurally similar BIGO´s (BIGO I and BIGO II) were deployed as described in detail by Sommer et al. (2009). In brief, each BIGO contained two circular flux chambers (internal diameter 28.8 cm, area 651.4 cm^2). A TV-guided launching system allowed smooth placement of the observatories at selected sites on the sea floor. Four hours after the observatories were placed on the sea floor the chambers were slowly driven into the sediment (~ 30 cm h^{-1}). During this initial time period where the bottom of the chambers was not closed by the sediment, the water inside the flux chamber was periodically replaced with ambient bottom water. The water body inside the chamber was replaced once more with ambient bottom water after the chamber has been driven into the sediment to flush out solutes that might have been released from the sediment during chamber insertion. To trace nitrogen fluxes (NO_3^-, NO_2^-, NH_4^+), iron, phosphorous and silicate release as well as total alkalinity 8 sequential water samples were removed with a glass syringe (volume of each syringe ~ 47 ml) by means of glass syringe water samplers. The syringes were connected to the chamber using 1 m long Vygon tubes with a dead volume of 5.2 ml. Prior to deployment these tubes were filled with distilled water. Another 4 water samples were taken from inside the benthic chamber using a peristaltic pump, which slowly filled glass tubes. These samples were used for the gas analyses of N_2, Ar and pCO_2. To monitor the ambient bottom water an additional syringe water sampler was employed and another series of four glass tubes were used. The positions of the sampling ports were about 30 – 40 cm above the sediment water interface. O_2 was measured inside the chambers and in the ambient seawater using optodes (Aandera) that were calibrated before each lander deployment.

Six deployments of BIGO-I and BIGO-II were conducted (see. Fig. 3.2, station list section 7) at the main sites at the 12°S working area in water depths of about 70, 150, 250, 400, 750, and 1000 m. At these sites microbiological (see section 5.4.4) porewater geochemistry (see section 5.4.1), profiling studies (see section 5.4.3) as well as Fe measurements (see section 5.3.3) were conducted. In addition four in situ flux measurements were carried out at the following sites in between the main stations: BIGO-II-1 (306 m), BIGO-II-4 (128 m), BIGO-I-4 (195m), and BIGO-I-5 (101 m). We deviated from the proposed plan to make further flux measurements at different locations further south and north of the 12°S working area. This was due to the interesting finding of sulfidic bottom water conditions that was depleted in NO_3^- and NO_2^- at the shallow shelf at 12°S, which was not encountered during our previous M77-1 cruise within the 1st phase of the SFB 754. Although not finally corrected, preliminary fluxes show that specifically the shallow shelf sediments that were covered with sulphide oxidizing bacterial mats represented an important site for the release of ammonium and TPO_4, Fig. 5.4.2.1. The magnitude of TPO_4 and ammonium release was much higher than compared to fluxes measured during the M77-1 cruise in 2008 at 11°S.

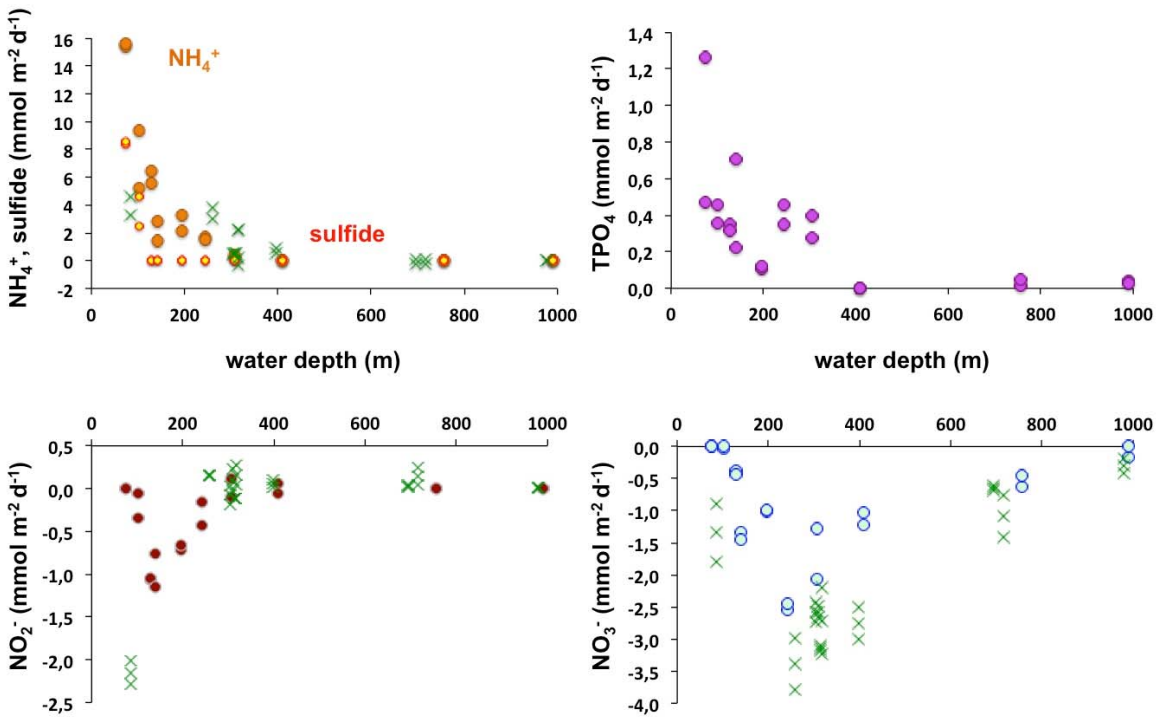

Fig. 5.4.2.1 In situ fluxes of NH_4^+, sulphide, NO_3^-, NO_2^- and TPO_4 measured using benthic lander along the depth transect at 12°S. The green crosses denote fluxes of the respective species during M77-1 at 11°S. Flux data for M77-1 from Bohlen et al. (2011), Noffke et al. (2012), Sommer et al. (unpubl. data), Glock et al. (2013). Note these fluxes are preliminary and not finally corrected. Positive values denote a flux from the sediment to the water column and vice versa.

5.4.3 Profiling flux measurements

M. Larsen, A. Glud

To complement the area-integrated flux measurements carried out by the BIGO landers (see section 5.4.2), we used microelectrodes to investigate small-scale heterogeneity in distribution and concentrations of electron donors and resulting fluxes across the sediment-water interface. Measured micro-profiles provide important information on carbon and nitrogen mineralization processes and help constraining sediment horizons characterized by different diagenetic pathways. Furthermore micro-profiles provide insight in the role of fauna-mediated solute transports compared to diffusion-mediated transport.

Using a transecting profiler (Glud et al. 2009) we determined micro-profiles of O_2, NO_3^- and N_2O in the surface sediments along the depth transect, at 6 stations with water depths of about 150, 250, 650, 750, and 1000 m, respectively. At depths of 150, 250, 750 and 1000 m the profiling lander was deployed simultaneously with the BIGO landers (see section. 5.4.2). At each station 20 to 100 individual profiles were measured. The transecting profiler was equipped with a total of 10 microelectrodes for O_2, NO_3^-, N_2O and resistivity (typically 3 O_2, 3 NO_3^-, 2 N_2O and 2 resistive sensors). The lander was positioned on the seafloor using a TV-guided launching system, allowing visual observation of the sea floor at the deployment position. Two hours after

the lander had been positioned a measurement routine was initiated with an automatic surface detection step (using signals of the resistivity sensors) that positioned the microelectrodes 3 cm above the sediment surface. From the initial position the microelectrodes were stepwise driven vertically into the sediment, with a step size of 300 µm, reaching a maximum depth of 5 cm. At each depth the microelectrode signals was logged after a resting time of 60 sec. After the microelectrodes had reached the maximum depth, the sensors were moved back to the initial position 3 cm above the sediment surface. The microelectrode were then moved 12 mm in the horizontal direction before the sensors were again lowered down into the sediment. For each deployment this routine was repeated 5 to 10 times. The lander was furthermore equipped with a Niskin bottle to collect bottom water for of O_2, DIC and NO_3^- concentrations. At each station microelectrode profiles were additionally measured ex situ in recovered sediment cores on board the ship. Preliminary data show that as expected O_2 was fully depleted at the shallow stations (150 and 250 m) but on the outer stations the average O_2 penetration depth increased from 2.1 mm (SD=0.6 mm) at 650 m to 3.2 mm (SD=0.4) at the 750 m to a maximum depth of 4.2 mm (SD=0.9 mm) at the 1000 m station.

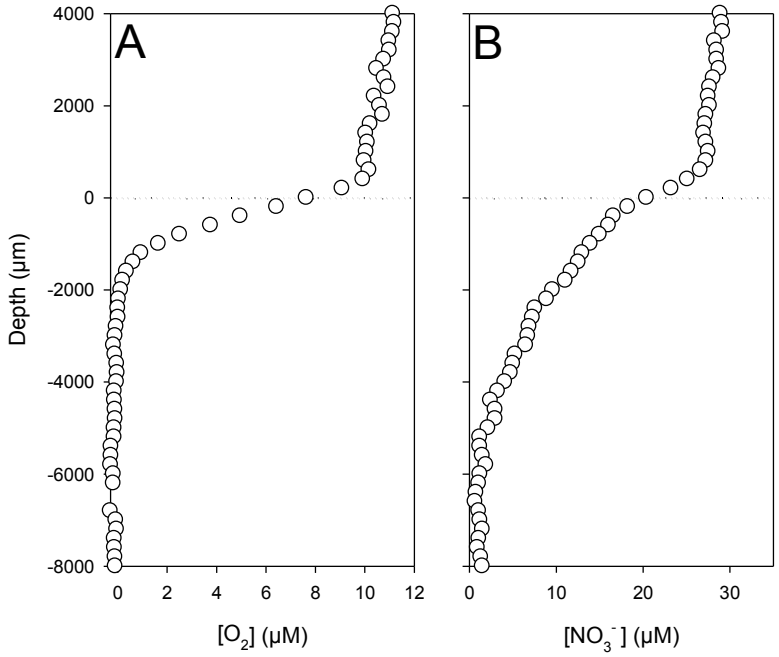

Fig. 5.4.3.1 Typical microelectrode profiles measured with the in situ profiling lander from the 650 m station A) O_2 microprofile and B) NO_3^- microprofile. Bottom water sensor signals were calibrated against water samples collected with a CTD water sampling rosette.

5.4.4. Microbiology of nitrogen fixation and associated processes

T. Treude, J. Gier, J. Schweers, G. Schüßler

Objectives

The aim of this study was to quantify benthic nitrogen fixation in surface sediments inside and outside the Peruvian oxygen minimum zone, i.e., along a depth transect, as well as to identify the responsible organisms and coupled metabolic processes, such as denitrification, bacterial sulfate and iron reduction and methanogenesis. Nitrogen fixation and denitrification rates will be incorporated into benthic nitrogen budgets gained from benthic lander experiments (see section 5.4.2 S. Sommer et al.) to follow the fate of individual nitrogen species at the benthic boundary. Additionally, two ammonium experiments were conducted to determine at which ammonium concentration nitrogen fixation would be inhibited and to check whether ammonium is incorporated into cell biomass. Furthermore, rates of sulfate and iron reduction as well as methanogenesis will be used to quantify organic matter degradation in sediments along depth gradients.

Sampling and on-board incubations

Sediment-sampling
Sediment samples were taken either by multicoring, gravity coring or from a benthic chamber of the BIGO lander system (see section 5.4.2 S. Sommer et al.). Samples from multicoring were used as follows: (1) one core for nitrogen fixation rate analyses (acetylene reduction method, see below), CAtalyzed Reporter Deposition Fluorescence In Situ Hybridization (CARD-FISH), and RNA/DNA analyses, (2) six cores for denitrification rate measurements (acetylene inhibition method, see below), (3) one core (two sub-cores) for sulfate reduction rate measurements (radiotracer method, see below), (4) two cores for iron reduction rate measurements (DIC method, see below), (5) one core for gas profiling (CH_4, N_2O, measured on GC, see below), (5) one core for methanogenesis rate measurements (increase in headspace methane concentration via GC, see below). Gravity core samples were used for methanogenesis (radiotracer method, see below). Samples from the benthic chamber were used as follows: (1) one core for nitrogen fixation rate analyses (acetylene reduction method, see below), CARD-FISH, and RNA/DNA analyses, (2) three cores for denitrification rate measurements (acetylene inhibition method, see below), (3) one core (three sub-cores) for sulfate reduction rate measurements (radiotracer method, see below), (3) one core for iron reduction rate measurements (DIC method, see below). At two stations, a replicate multicore core was used for $^{15}N_2$-determination of nitrogen fixation rates and two ammonium incubation experiments (see below). All sampling details are provided in Table 5.4.4.1.

Table 5.4.4.1 Sediment sampling details for denitrification (DNF; $^{15}N_2$-labelling = ^{15}N-DNF), methanogenesis (MG; ^{14}C-labelling = ^{14}C-MG), nitrogen fixation (nitrogenase activity via acetylene reduction = NA; $^{15}N_2$-labelling = ^{15}N-Fix), nitrogen fixation and labeled ammonium ($^{15}NH_4^+$ -Fix), nitrogen fixation and ammonium (NA+NH_4^+), sulfate reduction, iron reduction, CARD-FISH, and RNA/DNA analyses.

Station	Instrument	DNF	^{15}N-DNF	MG	^{14}C-MG	NA	^{15}N-Fix	$^{15}NH_4^+$-Fix	NA + NH_4^+	Sulfate reduction	Iron Reduction	CARD-FISH/ RNA/DNA
17	MUC 5	X		X						X	X	X
18	MUC 6					X						
36	MUC 10	X		X						X	X	X
37	MUC 11					X						
55	MUC 13	X		X		X				X	X	X
85	BIGO 1-1	X				X				X	X	X
86	MUC 17					X				X	X	X
87	MUC 18	X		X								
97	BIGO 2-2	X				X				X	X	X
107	MUC 23					X				X	X	X
108	MUC 24	X										
131	BIGO 1-2	X				X				X	X	X
143	BIGO 2-3	X				X				X	X	X
155	MUC 28					X				X	X	X
156	MUC 29	X										
173	BIGO 1-3	X				X				X	X	X
177	MUC 32						X	X	X			
199	MUC 35	X										
218	MUC 37	X										
219	MUC 38		X				X	X	X			
232	BIGO 2-5	X				X				X	X	X
254	GC 3				X							
268	GC 8				X							
288	CTD 84									X		X

Nitrogen fixation rates: sampling and incubations

At selected stations (Table 5.4.4.1), one multicorer core was used for the determination of nitrogen fixation rates (acetylene reduction assay (Capone, 1993)), CARD-FISH (Pernthaler et al., 2002), and RNA/DNA for later qPCR analyses (sediment frozen at -80°C). The following sampling scheme was used: 0–6 cm sediment depth in 1-cm intervals, 6–10 cm sediment depth in 2-cm intervals, and 10–20 cm sediment depth in 5-cm intervals. Push cores from the benthic chamber of the BIGO lander system (Table 1) were sliced in 5 cm intervals (0-15 cm). For determination of nitrogen fixation rates, 10 cm^3 sediment per interval were added into 60 ml serum vials (triplicates) and crimp sealed under N_2 atmosphere. After this 5 ml C_2H_2 were injected. The acetylene reduction assay was followed over a week (4-5 time points including time-zero) on a gas chromatograph with a flame ionization detector onboard. For this purpose, 100 µl of the headspace were injected into the gas chromatograph. Samples were kept in the dark and under in situ temperature (9°C, based on CTD data). Finally, nitrogen fixation rates were calculated with the conversion factor of $3C_2H_4$:$1N_2$ (Welsh et al., 1996).

At two stations (Table 5.4.4.1), one multicorer core was sliced according to the sampling scheme mentioned above and was used for an $^{15}N_2$ incubation experiment (Holtappels et al., 2011). Therefore, 10 cm^3 sediment per depth were added to a 15 ml serum vial (4 replicates) and filled up with anoxic seawater collected from supernatant of the multicorer core. The vials were crimp

sealed air bubble-free and two replicates per depth were injected with 300 µl $^{15}N_2$ while the other two replicates served as control without $^{15}N_2$ injection. In the home laboratory two replicate samples (1 including $^{15}N_2$ and 1 without) will be collected at two time points (12 and 16 weeks) for later determination of $\delta^{15}N$ on a mass spectrometer. Furthermore, CARD-FISH samples will be collected for using Halogen In Situ Hybridization-Secondary Ion Mass Spectroscopy (HISH-SIMS) and to check for the incorporation of ^{15}N into the bacterial biomass. Samples for natural abundance will be dried in 2 ml tubes for analysis with a mass spectrometer.

Experiments to investigate whether elevated ammonium pore water concentrations inhibit benthic N_2-fixation

Multicorer cores for two ammonium experiments to investigate whether elevated ammonium levels inhibit N_2-fiaxtion were taken at the same stations as for the $^{15}N_2$ incubation experiment (Table 5.4.4.1). In the first experiment, different ammonium concentrations were added to sediment slurries and the nitrogenase activity via the acetylene reduction assay was examined, to determine at which ammonium concentration nitrogen fixation by benthic bacteria would be inhibited. Of each multicorer core, the top 5 cm were mixed and 9 cm^3 of the sediment were added to a 60 ml serum vial. Additionally, 3 ml anoxic seawater from the top of the sediment core were added and different ammonium concentrations were injected (triplicates of: 0, 100, 500, 1000, 2500, 4000, and 5000 µmol). The vials were crimp sealed under N_2 and injected with 5 ml C_2H_2. The procedure followed the protocol of the acetylene reduction assay as described above. In the second experiment, labeled ammonium ($^{15}NH_4^+$) was used to check whether bacteria incorporate ammonium into their biomass. At two stations, the top 5 cm of one core were mixed and 9 cm^3 of the sediment were transferred into 15 ml serum vials. The remaining volume was filled bubble-free with anoxic seawater and different $^{15}NH_4^+$ concentrations (500, 1000, 1500 µmol). Two replicates per concentration included $^{15}NH_4^+$ and two replicates did not contain $^{15}NH_4^+$. The further processing will follow the same procedure as described for the $^{15}N_2$ labeling experiment.

Determination of denitrification rates

For determining rates of denitrification with the acetylene inhibition method (Sørensen, 1978), the first two centimeters of multicorer cores were sliced in 1 cm- intervals. Per depth interval, 10 cm^3 sediment were sub-sampled into 30 ml serum vials in triplicates, resulting in 18 vials in total. For push cores taken from the benthic chamber of the BIGO system, the depth intervals 0-2 cm and 2-4 cm were used for sub-sampling. Per depth, six 15 ml- serum vials were filled with 5 cm^3 sediment, resulting in 18 vials at the end. All vials were closed under an N_2-atmosphere. Then, two approaches were prepared to determine denitrification rates: (1) amendment with 40 µM nitrate, (2) amendment with 500 µM nitrate. For both approaches, three treatments were prepared in triplicates: (1) plus nitrate for time point T_0, (2) plus nitrate for time point T_1 (after 24h), (3) plus nitrate and 10% per volume acetylene (~ 3 ml) for time point T_1 (after 24 hours). N_2O concentration in the sediment was measured using N_2O-microsensors (Unisense) on board (Revsbech et al., 1989; Binnerup et al., 1992). N_2O concentration of T_0-samples was measured directly after nitrate addition, T_1-samples were incubated for 24 hours at 9 °C prior to micro-sensor measurement.

After micro-sensor measurement, anoxic ultrapure water was added to the sediment samples to produce a sediment-slurry. The slurry was transferred into argon purged 50 ml- centrifuge tubes, then centrifuged at 4000 rpm for 30 minutes at 4°C. The supernatant was collected, filtered through a 0.2 µm filter and immediately frozen for later nitrate analysis in the home laboratory on land.

At one station two multicorer cores were used for ^{15}N-nitrate-incubation experiments. The cores were sliced in the same manner as above, using the depth intervals 0-1 cm and 1-2 cm for sub-sampling. After this, 6 cm^3 sediment were transferred to a 15 ml serum vial under a helium atmosphere, then 6 ml of anoxic deep water were added before closing with a butyl rubber stopper. 40 µM ^{15}N-nitrate was injected through the stopper and the reaction was stopped at 4 different time points by adding 100µl of a $HgCl_2$-solution through the stopper. The four time points were: 0, 12, 24, and 48 hours. Samples were stored upside down for later analysis of $^{15}N_2$ on a mass spectrometer back in the home laboratory.

Determination of methanogenesis: sampling and incubations

Rates of methanogenesis in sediment retrieved via the multiple corer were determined by measuring the increase of methane concentration in the headspace over time. For this purpose, one multicorer core per station was sliced in 5 cm intervals and 10 cm^3sediment were transferred into a 60 ml serum vial. The maximum sampling depth was 47 cm, resulting in 10 depth intervals. Under an N_2 atmosphere, 10 ml of anoxic deep water were added to the vial, and the slurry was mixed thoroughly before sealing with a butyl rubber stopper.

The first gas chromatographic measurement was done directly after preparation of the vials by injecting 100 µl of the headspace sample into a gas chromatograph (see above). The following measurements were done in 2-4 day-intervals depending on the methane concentration development in the headspace.

For the determination of methanogenesis rates via CO_2 reduction in gravity cores the ^{14}C-bikarbonate labeling experiments were conducted. The gravity core was sub-sampled at 10-12 different sediment depths, resulting in slice intervals of 20-33 cm. The maximum core length was 400 cm. First, 2 cm^3 sediment were transferred into a 15 ml - serum vial containing 5 ml of NaOH (2.5%). This sample was used for the analysis of the methane concentration in the sediment by gas chromatograph measurements. For CO_2 reduction, 5 cm^3 sediment was sampled in triplicates into glass tubes sealed with a syringe plunger (rubber head) on one end and with a butyl rubber stopper on the other end. Then, ^{14}C-bicarbonate-tracer (dissolved in water, injection volume = 6 µl = 222 kBq, specific activity = 1.85-2.22 GBq/mmol) was injected through the stopper. The vials were incubated for 48 hours at 9°C before the reaction was stopped by transferring the sediment into 20 ml NaOH (2.5%). The processing of the samples will proceed in the home laboratory.

Gas sampling

One multicorer core per station (see Table 5.4.4.1) was used for sediment gas profiling of methane (CH_4) and nitrous oxide (N_2O), to identify hot spots of denitrification and

methanogenesis. The core was sliced in 2 cm intervals until 20 cm depth, followed by 5 cm intervals until a maximum depth of 48 cm. Then, 2 cm^3 of sediment were transferred into a 15 ml vial containing 5 ml NaOH (2.5%), the vial was sealed and shaken thoroughly. Gas chromatograph analysis of gas concentration in the headspace will follow in the home laboratory using a FID-GC for determining the CH_4 concentration and an ECD-GC for N_2O.

Determination of sulfate reduction: sampling and incubations

Multicorer cores and benthic chambers were sub-sampled with 2 smaller subcores (internal diameter = 26 mm, length = 300 (MUC) and 200 (BIGO) mm), which were sealed with rubber stoppers. Carrier-free $^{35}SO_4^{2-}$ (dissolved in water, injection volume = 6 µl, activity = 120 kBq, specific activity = 37 TBq $mmol^{-1}$) was injected at 1 cm intervals according to the whole core injection method of (Jørgensen 1978). The cores were incubated in the dark at 9 °C for ca. 12-18 h. After incubation, sediment cores were sectioned into 1 cm intervals and transferred into 50 ml plastic centrifuge vials filled with 20 ml zinc acetate (20% w/w). Control samples were first fixed before addition of tracer. Further processing of the samples will proceed in the home laboratory.

In one case (Table 5.4.4.1), sulfate reduction rates were determined at 5 depths (10, 20, 50, 65, and 68 m) in water collected by CTD. Water was filled bubble-free into 15 ml hungate tubes and sealed with rubber stoppers. Carrier-free $^{35}SO_4^{2-}$ (dissolved in water, injection volume = 30 µl, activity = 600 kBq, specific activity = 37 TBq $mmol^{-1}$) was injected and the tubes were incubated for 24 hrs at 9°C. After incubation, the water was transferred into 50 ml plastic centrifuge vials filled with 3 g zinc acetate (solid). Control samples were first fixed before addition of tracer.

Determination of iron reduction: sampling and incubations

Iron reduction activity was measured indirectly by subtracting sulfate reduction activity from total dissolved inorganic carbon (DIC) production in anoxic sediments (Vandieken et al. 2006). Per station (see Table 5.4.4.1) two multicorer cores were sliced into 2-cm intervals in the upper 10 cm. Benthic chambers were sub-sampled with one sub-core (6 mm diameter). From this core the top 10 cm (or less if shorter) were used completely. Sediment was filled under a constant stream of N_2 into gastight plastic bags in a cold room (9°C). The incubation bags were closed (without gas phase) and incubated at 9°C. Over a period of 14 d, subsamples were withdrawn 5 times from each bag. Porewater from the bags was retrieved by a porewater press under N_2 pressure through GF/F filters. Porewater (0.5-1 ml) was acidified with 40µl 6M HCl to preserve samples for Fe^{2+} analyzes. For DIC analysis, 1.8 ml aliquots were collected in glass vials without headspace and capped with Viton septa; these were fixed with $HgCl_2$, and stored at 4°C until analysis. Sulfate reduction in the anoxic bags was determined at each sampling time point in subsamples incubated with 120 kBq $^{35}SO_4^{2-}$ radiotracer (see above) in 5 ml glass tubes. After ca. 12-18 hrs, the incubations were stopped with 20% Zn acetate (see above). Further processing of the samples will proceed in the home laboratory.

5.4.5 Ex situ N-turnover experiments

M. Larsen, A. Glud

To determine the importance of denitrification and anammox and their quantitative contribution to the total nitrogen turnover at different stations in the working area, ex situ ^{15}N tracer experiments were conducted. Sites where these experiments were conducted are indicated in the station list by "Inc (N-Exp)".

Denitrification was estimated using the Isotope Pairing Technique (Nielsen 1992). This technique relies on the addition of $^{15}NO_3^-$ and measuring the production of $^{29}N_2$ and $^{30}N_2$. Denitrification was measured at stations with water depths of 250, 650, 750 and 1000 m. Denitrification at the shallower stations was not measured due to the high abundance of NO_3^- accumulating filamentous bacteria, that would interfere with the principles for the IPT measurement. For denitrification measurements six sub-cores taken from the MUC core liners were used. The sub-cores (internal diameter: 5.1cm) were incubated at in situ temperature and O_2 concentrations before the $^{15}NO_3^-$ tracer was added and subsequently samples for $^{29}N_2$ and $^{30}N_2$ were taken. In addition to the IPT method we also estimated denitrification using the N_2/Ar technique. In parallel to sediment core incubations for determining denitrification, sediment fluxes of O_2, NO_3^-, NH_4^+ were also measured.

The potential role of anammox to total N_2 production was investigated in anoxic sediment slurries (Thamdrup and Dalsgaard 2002) with different amendments of $^{15}NH_4^+$, $^{15}NO_3^-$, $^{14}NH_4^+$ and $^{14}NO_3^-$, and subsequently measuring the production of $^{29}N_2$ and $^{30}N_2$ in the slurries. At each station 1-2 MUC cores liner were sampled and the top 4 cm (excluding any oxic sediment) were used for the determination of potential anammox. Potential anammox was measured on stations at water depths of 80, 150, 250, 300, 400, 650, 750 and 1000 m. At stations with a high bacterial biomass, potential anammox rates were determined from an upper sediment layer (1-2 cm) and a deeper layer with relative little bacterial biomass (3-4 cm). The mass spectrometer analyses are scheduled for the coming months so at present we do not have any preliminary insight on these experiments.

5.4.6 Foraminifera ecology

J.C.E. Fernández, E. Johnston, J. Salazar

Benthic foraminifera are a major group of organisms in marine sediments in terms of abundance, biomass and diversity. Particularly in OMZs they are important for biogeochemical processes and carbon cycling (Gooday et al. 1992). Therefore, the assessment of the community ecology is essential for a more accurate understanding of the ecosystem functioning of the Peruvian OMZ. The whole community was sampled from the upper layers of sediments retrieved using a multicorer from water depths of 80, 150, 250, 305, 400, 650, 750 and 1000 m along the 12°S transect. Two separated cores from each deployment (pseudo-replicates) were taken for benthic foraminifera, along with one or two other cores for organic matter analysis. A fifth core was

sampled for sediment visual characterization. In the benthic foraminifera cores, the first two centimeters were sliced into 0.5 cm intervals and then into 1 cm intervals down to five centimeters. All samples were stored in plastic jars and preserved in buffered formalin 4% for later staining with Rose Bengal 1g/l for the recognition of 'living' individuals according to Rathburn and Corliss (1994). The spatial variation of species abundance and microhabitat (vertical distribution into the sediment) will therefore be compared to organic matter proxies and pore water geochemistry (see section 5.4.1) as well as to the results of the microbiology working groups (see section 5.4.4) in order to obtain an optimal and adequate understanding of foraminiferal ecology. Moreover, it has been found recently that benthic foraminifera can store large amounts of intercellular NO_3^- and that the stored NO_3^- can be used for respiration through denitrification (Risgaard-Petersen et al. 2006), being potentially quantitatively important compared to microbial denitrification (Piña-Ochoa et al. 2010). At six stations at water depths of 80, 150, 250, 650, 750 and 1000 m along the 12°S working area we collected foraminifera to quantify the internal pool of NO_3^- as a function of species, size and vertical distribution in the sediment. At each station, sediment cores were sliced in 1 cm depth intervals (down to 5 cm). For each depth interval, foraminifera were sorted to species level and frozen for later analysis. The collected individuals will be used for determining the intracellular NO_3^- pool in the different species. From the encountered species a clear change was observed in species compositions from the shallow anoxic to the deeper oxic stations.

5.5 Expected Results

S. Sommer, shipboard scientific party

All planned measurements and investigations were conducted successfully. To achieve the scientific aims, oceanographical investigations, geochemical measurements in the water column and the benthos as well as microbiological studies were conducted coherently. For six selected sites along the depth transect at 12°S a complete data set is available from all scientific groups. Furthermore, this cruise was embedded into a series of other Pacific cruises M90, M91 and M93 that took place within the framework of the SFB754. From the combination of the different results of each discipline during M92 as well as with data from the other Pacific cruises we expect a high degree of synergy. This allows addressing the following key questions and problems that are central to the Kieler SFB754 and to research in oxygen minimum zones in general:

i. to assess potential feedback of benthic nutrient release on processes in the water column and primary productivity in the surface water. The source strength of nutrient release at different sites in response to variable bottom water O_2, NO_3^-, and NO_2^- conditions as well as availability of sedimentary organic carbon was intensively investigated in situ using state of the art benthic landers as well as pore water gradients. These results will be combined with in situ micro-profiling measurements of O_2, NO_3^- and N_2O. Particular focus was on in situ flux measurements at sulphide oxidizing microbial mat sites that were ubiquitous within a depth range of about 73 to about 300 m. Under transient bottom water O_2 conditions these organism are capable to strongly affect the nitrogen as well as phosphorous turnover. Furthermore samples from these sulphur bacteria were taken for later laboratory analyses;

ii. fluxes across the sediment water interface in combination with water column nutrient profiles, radiotracer profiles and hydrographical data as well as micro-structure turbulence data will allow to address the fate of nutrients once they are released from the seafloor. Major transport processes such as upwelling and vertical mixing of the nutrients to the surface mixed layer will be determined;

iii. microbiological studies conducted during the cruise in combination with ^{15}N labelling experiments, numerical modelling of pore water gradients as well as in situ fluxes will allow to identify the different processes involved in benthic carbon, N and P turnover and the release of nutrients into the bottom water. Measurements were conducted to determine whether fractionation by benthic organisms takes place during N turnover;

iv. during the previous M77 cruise as well as during this cruise extremely high TPO_4 release rates were measured particularly at the shelf and the upper slope which could not been explained by the input of P bound to organic matter, nor by the input of terrestrial P (Noffke et al. in prep.). High C/P ratios of organic matter in surface sediments of up to 516 indicated that organic P was severely depleted in organic matter relative to the Redfield ratio. If this material reflects the stoichiometry of the organic matter raining to the seafloor then mass balance calculations based on the benthic fluxes suggest that organic P can account for only a small fraction of the total particulate P input to the sediment inside the OMZ. Hence these authors speculate whether there is a further source of P, such as water column derived authigenic P, to these sediments. In order to better constrain organic carbon flux to the sediment as well as its elemental composition geochemical measurements (filter analysis from in situ pumps) as well as radiotracer geochemistry will be combined.

6 Ship's Meteorological Station

During the entire duration of the cruise the weather as well as the sea was fine allowing smooth operation of all scientific gears. The data of the shipboard meteorological station are available from the DWD as well as from the GEOMAR data storage centre.

7 Station list M92

Station	Gear No.	Date	Position		Time	Depth	Remarks
No.		2013	Lat. [°S]	Long. [°W]	[UTC]	[m]	
M92-1	CTD 1	05.01.	12°1.976'	77°39.992'	15:04	178	
M92-2	AMOP shield 1	05.01.	12°2.032'	77°39.958'	16:55	179	deployment failed
M92-3	AMOP shield 2	05.01.	12°2.031'	77°39.954'	18:29	177.5	
M92-4	AMOP Mooring 1	05.01.	12°1.983'	77°39.701'	21:30	180	
M92-5	CTD/RO 2	06.01.	12°18.575'	77°17.570'	17:50	143.7	
M92-6	MUC 1	06.01.	12°18.558'	77°17.565'	18:38	142	
M92-7	CTD/PO 3	06.01.	12°23.360'	77°24.114'	20:15	243.7	Many patches of sulfur bacteria; soft greenish sediment
M92-8	MUC 2	06.01.	12°23.340'	77°24.178'	20:42	249	Very soft sediment; lost sediment surface; not all cores retrieved; sulfidic smell; blackish-green; many sulfur bacteria; sometimes in dense round patches
M92-9	CTD/RO 4	06.01.	12°29.286'	77°32.272'	23:04	506	
M92-10	MUC 3	07.01.	12°29.284'	77°32.268'	00:02	505	Hard bottom; abundant, fish and spider crabs, no samples taken
M92-11	CTD/RO 5	07.01.	12°31.308'	77°34.953'	01:51	731	
M92-12	MUC 4	07.01.	12°31.308'	77°34.952	02:24	750.9	Polychaetes; octopus; fish; more a deep sea like surface with lots of Lebensspuren and bioturbation; surface sediment seems oxidized
M92-13	MB Bathymetry 1	07.01.	12°25.790'	77°25.715'	04:53		survey stopped at 12°25.568' °S and 77°27.177' °W; UTC 11:20
M92-14	GLIDER IFM 07	07.01.	12°17.000'	77°39.956'	13:10	878	
M92-15	GLIDER IFM 03	07.01.	12°18.500'	77°42.003'	14:26	1223	
M92-16	Multi Beam EM 122 2	07.01.	12°18.704'	77°25.625'	16:30	191	
M92-17	MUC 5	07.01.	12°23.321'	77°24.176'	17:44	253	Sulfur bacteria mat; dense; very soft sediment; Geochemistry MUC 1

Station	Gear No.	Date	Position		Time	Depth	Remarks
No.		**2013**	**Lat. [°S]**	**Long. [°W]**	**[UTC]**	**[m]**	
M92-18	MUC 6	07.01.	12°23.328'	77°24.184'	18:44	244	
M92-19	Mooring KPO 1100	07.01.	12°19.299'	77°25.170'	19:55	197	
M92-20	GoFlo 1	07.01.	12°25.0'	77°26.0'	20:30	302	cancelled due to technical problems
M92-21	GoFlo 2	07.01.	12°25.0'	77°26.0'	22:50	302	resumed work of station 21, after technical problems; issues with GoFlo were resolved; bottles were not "fired" because of problems with messenger weights
M92-22	Bathymetrie 3	08.01.	12°25.157'	77°26.126'	00:45		survey stopped at 12°23.7' °S and 77°23.8' °W; UTC 12:44
M92-23	MUC 7	08.01.	12°23.293'	77°24.204'	13:15	243	Beggiatoa/Thioploca *Inc (N-exp)*
M92-24	MUC 8	08.01.	12°23.293'	77°44.204'	14:09	243	*Inc (N-exp)*
M92-25	CTD/RO 6	08.01.	12°24.904'	77°26.314'	15:09	305	Nutrients
M92-26	MUC 9	08.01.	12°24.903'	77°26.301'	15:50	305	similar to 250 m; patchy with mats
M92-27	Multibeam 4	08.01.	12°25.00'	77°26.44'	16:42	308	
M92-28	Multibeam 5	08.01.	12°23.13'	77°28.37'	17:59	298	
M92-29	Mooring KPO 1101	08.01.	12°23.66'	77°27.43'	18:39	302	
M92-30	BIGO-II-1	08.01.	12°24.905'	77°26.296	22:24	305.5	Deployment
M92-31	GoFlo 3	08.01.	12°23.0'	77°24.0'	23:26	244	
M92-32	CTD/RO 7	09.01.	12°23.302'	77°24.214'	00:40	244.7	
M92-33	Bathymetry MB-profile KPO 1101 6	09.01.	12°23.302'	77°24.214'	01:04	245	EM 710 was recording and pinning from 01:45 UTC to 02:25 UTC together with EM 122; Data are stored in "KPO1101"-file; 10:33 UTC end of recording; 12°13.230' °S and 77°10.123' °W, depth 75 m
M92-34	Satellite Mini Lander SLM2-1	09.01.	12°29.21'	77°32.11'	13:02	497	beacon weak signal
M92-35	POZ-Lander 2	09.01.	12°24.815'	77°26.032'	15:44	298	
M92-36	MUC 10	09.01.	12°18.708'	77°17.794'	18:22	145	
M92-37	MUC 11	09.01.	12°18.708'	77°17.795'	18:55	144	

Station	Gear No.	Date	Position		Time	Depth	Remarks
No.		2013	Lat. [°S]	Long. [°W]	[UTC]	[m]	
M92-38	CTD/RO 8	09.01.	12°23.336'	77°24.191'	20:16	244.8	
M92-39	In situ pumps 1	09.01.	12°23.337'	77°24.190'	21:25	245	cancelled due to technical problem; McLane pump clamps too small
M92-40	In situ pumps 2	09.01.	12°23.337'	77°24.192'	23:30	244.5	
M92-41	CTD 9	10.10.	12°13.54'	77°10.52'	03:45	72	
M92-42	MUC 12	10.01.	12°13.509'	77°10.513'	04:08	73.6	
M92-43	Glidertest/Bathymetry survey 3	10.01.	12°21'	77°40'	07:04	1106	survey M92-3; 08:16 UTC (12°28' °S / 77°40' °W) stop recording due to high maritime traffic (change of course); 08:50 UTC (12°28' °S / 77°40' °W) Logging again; 08:57 UTC (12°28' °S / 77°40' °W) take another way because of too many fisherboats; End 12:00 UTC (12°17.084' °S / 77°21.618' °W), depth 165 m
M92-44	BIGO-2-1	10.01.	12°25.01'	77°26.31'	13:21		Recovery
M92-45	CTD/RO 10	10.01.	12°41.18'	77°48.88'	15:54	1723,7	
M92-46	Multibeam 7	10.01.	12°39.69'	77°48.82'	17:42	1581.5	end survey: 12°41.82' °S and 77°49.38' °W; depth: 1849.9 m
M92-47	Mooring KPO 1103 4	10.01.	12°40.95'	77°48.90'	19:15	1700	
M92-48	MSS 1	11.01.	12°34.003'	77°38.796'	00:08	990	
M92-49	CTD/RO 11	11.01.	12°34.863'	77°38.954'	01:31	1002.5	Nutrients
M92-50	In situ pumps 3	11.01.	12°34.863'	77°38.955'	02:22	1026.5	
M92-51	MSS 2	11.01.	12°30.455'	77°34.495'	07:00	750	
M92-52	CTD/RO 12	11.01.	12°31.406'	77°35.193'	08:58	773	
M92-53	CTD/RO 13	11.01.	12°29.201'	77°32.084'	10:13	497.2	
M92-54	MUC 13	11.01.	12°13.497'	77°10.515'	13:26	70	Very turbid; weight not visible on the way down; bacteria on sediment visible, when the MUC was in

Station	Gear No.	Date	Position		Time	Depth	Remarks
No.		**2013**	**Lat. [°S]**	**Long. [°W]**	**[UTC]**	**[m]**	
							sediment
M92-55	MUC 14	11.01.	12°13.496'	77°10.515'	13:56	70	
M92-56	In situ pumps 4	11.01.	12°18.696'	77°17.790'	15:07	150	
M92-57	BIGO-I-1	11.01.	12°18.711'	77°17.803'	19:09	141.5	Deployment
M92-58	Profiler 1	11.01.	12°18.738'	77°17.810'	21:23	141	Deployment
M92-59	SLM 3	11.01.	12°13.487'	77°10.530'	22:45	76	
M92-60	GoFlo 4	12.01.	12°18.7'	77°18.0'	00:09	145	
M92-61	CTD 14	12.01.	12°18.697'	77°18.004'	01:01	145.5	Nutrients
M92-62	MUC 15	12.01.	12°18.696'	77°18.004'	01:40	146	*Inc (N-exp)*
M92-63	CTD 15	12.01.	12°27.196'	77°29.501'	03:20	406	Nutrients
M92-64	MSS 3	12.01.	12°27.196'	77°29.591'	03:55	406	04:14 bottom contact
M92-65	MSS 4	12.01.	12°27.196'	77°29.500'	06:34	408	
M92-66	CTD/RO 16	12.01.	12°27.535'	77°29.593'	07:23	414	
M92-67	MSS 5	12.01.	12°29.22'	77°32.10'	08:42	497.7	
M92-68	CTD/RO 17	12.01.	12°29.222'	77°32.106'	09:58	497	Nutrients
M92-69	MUC 16	12.01.	12°14.897'	77°12.707'	12:55	103	
M92-70	In situ pumps 5	12.01.	12°13.493'	77°10.807'	14:30	74.2	
M92-71	CTD 18	12.01.	12°13.5'	77°10.8'	16:45	74	
M92-72	GoFlo 5	12.01.	12°13.5'	77°10.8'	17:17	74	
M92-73	BIGO-II-2	12.01.	12°23.305'	77°24.192'	20:01	243.9	deployment failed; cancelled due to technical problems; releaser failed
M92-74	BIGO-II-2	12.01.	12°23.300'	77°24.186'	21:08	243.8	deployment from station 73 repeated
M92-75	SLM 4	12.01.	12°18.732'	77°17.812'	22:34	148	
M92-76	CTD/RO 19	12.01.	12°21.493'	77°21.699'	23:49	188	Nutrients
M92-77	MSS 6	13.01.	12°21.773'	77°21.920'	00:29	200	
M92-78	MSS 7	13.01.	12°20.841'	77°21.632'	02:21	200	
M92-79	CTD 20	13.01.	12°20.089'	77°19.680'	04:15	169.1	
M92-80	MSS 8	13.01.	12°19.546'	77°19.567'	05:01	170	
M92-81	MSS 9	13.01.	12°19.029'	77°19.537'	06:44	160	
M92-82	CTD/RO 21	13.01.	12°23.287'	77°24.226'	08:30	244	
M92-83	MSS 10	13.01.	12°22.850'	77°24.107'	09:16	240	
M92-84	CTD/RO 22	13.01.	12°24.788'	77°25.992'	10:27	297	
M92-85	BIGO-I-1	13.01.	12°18.703'	77°17.912'	13:08	145	Recovery
M92-86	MUC 17	13.01.	12°31.395'	77°35.211'	15:15	774	Holothurians; soft sediment; no Thioploca mats; bioturbation, asteroids
M92-87	MUC 18	13.01.	12°31.373'	77°35.184'	16:45	769.4	
M92-88	Profiler 1	13.01.	12°18.56'	77°17.82'	20:00		Recovery
M92-89	MUC 19	13.01.	12°18.699'	77°17.807'	21:19	144	
M92-90	MUC 20	13.01.	12°18.704'	77°17.808'	21:59	145	
M92-91	CTD 23	13.01.	12°18.775'	77°17.824'	22:30	144	Nutrients

Station	Gear No.	Date	Position		Time	Depth	Remarks
No.		2013	Lat. [°S]	Long. [°W]	[UTC]	[m]	
M92-92	CTD 24	13.01.	12°23.30'	77°24.20'	23:44	244.2	
M92-93	MUC 21	14.01.	12°27.199	77°29.513'	00:58	410	possibly foraminiferal sands on video image
M92-94	MSS 11	14.01.	12°25.742'	77°28.161'	02:10	350	
M92-95	CTD/RO 25	14.01.	12°26.305'	77°28.211'	04:40	355.7	
M92-96	Bathymetry survey 8	14.01.	12°24.661'	77°25.123'	05:53	282	Logging file: M92-4; restart system about 8:15 UTC; end survey 11:38 UTC
M92-97	BIGO-II-2	14.01.	12°24.360'	77°24.300'	13:15	246.4	Recovery
M92-98	CTD 26	14.01.	12°13.504'	77°10.799'	17:00	75.1	
M92-99	MB 9	14.01.	12°22.19'	77°20.14'	18:30	190.4	End survey: 12°22.35' °S and 77°21.68' °W, 19:30 UTC
M92-100	Mooring 5	14.01.	12°23.71'	77°20.20'	20:26	207.6	
M92-101	MUC 22	14.01.	12°31.393'	77°35.202'	23:11	774	Cores for foraminifera *Inc (N-exp)*
M92-102	GoFlo 6	15.01.	12°31.3'	77°35.3'	01:00	774	
M92-103	CTD 27	15.01.	12°31.327'	77°35.265'	03:23	772.7	Nutrients
M92-104	MSS 12	15.01.	12°31.327'	77°35.264'	04:10	772.4	
M92-105	CTD/RO 28	15.01.	12°13.604'	77°10.937'	09:42	77.1	Nutrients
M92-106	MSS 13	15.01.	12°13.604'	77°10.937'	10:30	76.3	
M92-107	MUC 23	15.01.	12°27.199'	77°29.497'	13:05	407	
M92-108	MUC 24	15.01.	12°27.197'	77°29.497'	13:54	407	
M92-109	Glider	15.01.	12°20.12'	77°34.92'	15:36	415.5	
M92-110	BIGO-I-2	15.01.	12°13.506'	77°10.793'	19:27	74	Deployment
M92-111	CTD 29	15.01.	12°18.729'	77°17.757'	20:57	144.5	
M92-112	GoFlo 7	15.01.	12°24.8'	77°26.0'	22:25	298	
M92-113	In situ pumps 6	16.01.	12°23.304'	77°24.196'	00:30	243	
M92-114	CTD/RO 30	16.01.	12°23.30'	77°24.20'	03:17	243.8	
M92-115	CTD/RO 31	16.01.	12°23.304'	77°24.196'	04:10	244	Nutrients
M92-116	MSS 14	16.01.	12°22.781'	77°24.160'	04:40	231.1	
M92-117	MSS 15	16.01.	12°20.776'	77°21.734'	07:33	200	
M92-118	CTD/RO 32	16.01.	12°21.503'	77°21.722'	09:28	194.3	Nutrients
M92-119	CTD 33	16.01.	12°31.398'	77°35.196'	12:55	772.3	
M92-120	MUC 25	16.01.	12°31.397'	77°35.195'	13:53	773	MUCs for Annie Glud *Inc (N-exp)*
M92-121	MUC 26	16.01.	12°31.397'	77°35.196'	15:01	773	
M92-122	Glider IFM 12 1	16.01.	12°34.04'	77°32.00'	16:48	734.2	Cancelled due to defect rubber boat
M92-123	Glider IFM 12 1	16.01.	12°34.02'	77°32.03'	18:44	739.3	
M92-124	BIGO-II-3	16.01.	12°31.366'	77°34.997'	20:22	756	Deployment
M92-125	Profiler 2	16.01.	12°31.438'	77°34.961'	23:12	757	Deployment

Station	Gear No.	Date	Position		Time	Depth	Remarks
No.		**2013**	**Lat. [°S]**	**Long. [°W]**	**[UTC]**	**[m]**	
M92-126	GoFlo 8	17.01.	12°35.9'	77°41.7'	01:30	1022	Winch counter not working properly; 80 m difference to each sounder
M92-127	CTD/RO 34	17.01.	12°37.82'	77°44.14'	03:58	1194	Nutrients
M92-128	MSS 16	17.01.	12°28.485'	77°31.809'	06:30	480	
M92-129	CTD/RO 35	17.01.	12°29.194'	77°31.918'	08:10	493	Nutrients
M92-130	MSS 17	17.01.	12°26.391'	77°29.383'	09:29	400	
M92-131	BIGO-I-2	17.01.	12°13.528'	77°11.133'	13:48	76.8	Recovery
M92-132	CTD 36	17.01.	12°18.675'	77°17.845'	14:44	144	
M92-133	In situ pumps 7	17.01.	12°18.675'	77°17.845'	16:10	150	
M92-134	Glider IFM 11	17.01.	12°30.43'	77°27.25'	18:50	423.5	
M92-135	GoFlo 9	17.01.	12°27.2'	77°29.5'	20:50	407	at rope length 380 m rope tension dropped from 0,84 kN to 0,3 kN; probably contact with sea floor
M92-136	MUC 27	17.01.	12°27.185'	77°29.508'	23:02	408	*Inc (N-exp)*
M92-137	In situ pumps 8	18.01.	12°21.356'	77°29.507'	00:27	400	
M92-138	CTD/RO 37	18.01.	12°27.35'	77°29.5'	03:22	400	
M92-139	MSS 18	18.01.	12°14.238'	77°12.876'	06:08	110	
M92-140	CTD/RO 38	18.01.	12°14.908'	77°12.715'	08:05	100	Nutrients
M92-141	MSS 19	18.01.	12°15.873'	77°15.890'	09:05	130	
M92-142	CTD/RO 39	18.01.	12°16.495'	77°15.891'	09:53	130	Nutrients
M92-143	BIGO-II-3	18.01.	12°31.348'	77°34.975'	13:11	756	Recovery
M92-144	In situ pumps 9	18.01.	12°31.183'	77°35.093'	13:45	750	
M92-145	Glider IFM 06 1	18.01.	12°33.56'	77°32.46'	17:30	730	
M92-146	Profiler 2	18.01.	12°31.42'	77°35.14'	18:31		Recovery
M92-147	Mooring KPO 1102	18.01.	12°30.82'	77°34.82'	19:40	707	
M92-148	CTD/RO 40	18.01.	12°31.427'	77°34.957'	20:44	755	
M92-149	MSS 20	18.01.	12°31.491'	77°34.833'	21:40	750	
M92-150	CTD/RO 41	19.01.	12°36.599'	77°42.999'	00:59	1085	Nutrients
M92-151	MSS 21	19.01.	12°36.682'	77°42.963'	02:16	1095	
M92-152	CTD/RO 42	19.01.	12°38.586'	77°45.633'	05:41	1340	Nutrients
M92-153	MSS 22	19.01.	12°38.651'	77°45.585'	06:59	1350	
M92-154	CTD/RO 43	19.01.	12°41..517'	77°51.026'	09:23	2018	Nutrients
M92-155	MUC 28	19.01.	12°35.396'	77°41.000'	13:01	1025	Ophuiriods, sea urchins, asteroids; bottom survey: pull with 0,3kn in direction of 53°NE
M92-156	MUC 29	19.01.	12°35.377'	77°40.976'	14:35	1024	
M92-157	In situ pumps 10	19.01.	12°31.4'	77°35.2'	16:56	750	
M92-158	CTD 44	19.01.	12°31.385'	77°35.209'	20:42	772	
M92-159	BIGO-I-3	19.01.	12°34.911'	77°40.365'	22:16	989	Deployment

Station	Gear No.	Date	Position		Time	Depth	Remarks
No.		2013	Lat. [°S]	Long. [°W]	[UTC]	[m]	
M92-160	Multi Beam 10	20.01.	12°34.69'	77°45.58'	00:42	1002.8	Deployment
M92-161	Profiler 3	20.01.	12°35.402'	77°41.306'	13:24	1011	Deployment
M92-162	CTD 45	20.01.	12°35.404'	77°41.013'	15:01	1025	
M92-163	MUC 30	20.01.	12°35.404'	77°41.013'	16:34	1024	*Inc (N-exp)*
M92-164	MUC 31	20.01.	12°35.404'	77°41.008'	17:55	1026	*Inc (N-exp)*
M92-165	BIGO-II-4	20.01.	12°16.690'	77°14.995'	22:04	128.4	Deployment
M92-166	In situ pumps 11	20.01.	12°13.489'	77°10.805'	23:30	80	
M92-167	CTD/RO 46	21.01.	12°13.488'	77°10.804'	01:50	80	Nutrients
M92-168	MSS 23	21.01.	12°13.488	77°10.804'	02:38	80	
M92-169	MSS 24	21.01.	12°16.759'	77°15.020'	04:45	125	
M92-170	CTD/RO 47	21.01.	12°17.346'	77°15.108'	06:36	130	Nutrients
M92-171	MSS 25	21.01.	12°19.643'	77°19.922'	07:58	170	
M92-172	CTD/RO 48	21.01.	12°20.238'	77°19.896'	08:44	173	Nutrients
M92-173	BIGO-I-3	21.01.	12°34.91'	77°40.45'	12:36	988	Recovery
M92-174	CTD 49	21.01.	12°35.4'	77°41.0'	13:39	1025	
M92-175	In situ pumps 12	21.01.	12°35.400'	77°41.002'	15:00	1026.1	
M92-176	Profiler 3	21.01.	12°35.286'	77°41.432'	18:06		Recovery
M92-177	MUC 32	21.01.	12°27.215'	77°29.539'	20:13	409	
M92-178	MUC 33	21.01.	12°23.285'	77°24.217'	21:45	244	*Inc (N-exp)*
M92-179	CTD 50	21.01.	12°23.604'	77°23.911'	22:51	245	
M92-180	In situ pumps 13	21.01.	12°23.603'	77°23.911'	21:30	246	
M92-181	CTD 51	22.01.	12°23.603'	77°23.911'	02:56	245	Nutrients
M92-182	MSS 26	22.01.	12°22.534'	77°23.935'	03:38	250	
M92-183	MSS 27	22.01.	12°22.014'	77°23.413'	05:38	225	
M92-184	CTD/RO 52	22.01.	12°23.329'	77°23.391'	07:03	233	Nutrients
M92-185	MSS 28	22.01.	12°20.501'	77°21.718'	08:10	200	
M92-186	CTD/RO 53	22.01.	12°21.534'	77°21.698'	09:23	196	Nutrients
M92-187	BIGO-II-4	22.01.	12°16.77'	77°15.08'	12:50	129.1	Recovery
M92-188	In situ pumps 14	22.01.	12°16.732'	77°15.097'	14:00	129	
M92-189	Profiler 4	22.01.	12°23.600'	77°23.900'	18:39	245	Deployment
M92-190	GoFlo 10	22.01.	12°31.3'	77°35.2'	20:30	775	
M92-191	In situ pumps 15	22.01.	12°27.189'	77°29.500'	23:51	408	
M92-192	CTD/RO 54	23.01.	12°27.188'	77°29.499'	02:23	407	
M92-193	MSS 29	23.01.	12°27.188'	77°29.498'	03:00	400	
M92-194	MSS 30	23.01.	12°25.248'	77°28.221'	05:11	350	
M92-195	CTD/RO 55	23.01.	12°26.270'	77°28.348'	06:39	363	Nutrients
M92-196	MSS 31	23.01.	12°24.384'	77°25.776'	07:49	300	
M92-197	CTD/RO 56	23.01.	12°24.885'	77°25.845'	08:30	296	Nutrients
M92-198	MUC 34	23.01.	12°23.300'	77°24.230'	18:46	243.9	
M92-199	MUC 35	23.01.	12°23.302'	77°24.222'	19:22	244.6	*Inc (N-exp)*
M92-200	CTD 57	23.01.	12°23.350'	77°24.222'	20:09	245.7	
M92-201	BIGO-I-4	23.01.	12°21.502'	77°21.712'	21:19	195	Recovery
M92-202	Profiler 4	23.01.	12°23.43'	77°23.94'	22:23	243.9	Recovery
M92-203	MB 11	24.01.	12°12.887'	77°11.051'	00:02	75	
M92-204	In situ pumps 16	24.01.	12°30.326'	77°33.845'	13:15	600	
M92-205	CTD 58	24.01.	12°30.326'	77°33.856'	16:33	603.7	

Station	Gear No.	Date	Position		Time	Depth	Remarks
No.		**2013**	**Lat. [°S]**	**Long. [°W]**	**[UTC]**	**[m]**	
M92-206	Glider IFM 08	24.01.	12°33'	77°34'	18:00	600	
M92-207	BIGO-II-5	24.01.	12°27.207'	77°29.517'	19:37	409	Deployment
M92-208	MUC 36	24.01.	12°25.588'	77°25.203'	20:54	296	Without video control *Inc (N-exp)*
M92-209	Profiler 5	24.01.	12°35.380'	77°40.995'	23:08	1023	Deployment
M92-210	CTD 59	25.01.	12°35.434'	77°41.033'	00:31	1024	
M92-211	In situ pumps 17	25.01.	12°27.21'	77°29.52'	02:46	408.5	
M92-212	GoFlo 11	25.01.	12°18.9'	77°17.5'	07:07	144	
M92-213	MSS 32	25.01.	12°14.177'	77°11.898'	08:35	90	
M92-214	CTD 60	25.01.	12°14.684'	77°12.189'	09:29	96	Nutrients
M92-215	MSS 33	25.01.	12°14.684'	77°12.192'	10:01	95	
M92-216	CTD 61	25.01.	12°21.386'	77°21.751'	12:52	193.9	
M92-217	BIGO-I-4	25.01.	12°21.469'	77°21.694'	13:42	195.3	Recovery
M92-218	MUC 37	25.01.	12°13.503'	77°10.111'	15:47	71	
M92-219	MUC 38	25.01.	12°13.518'	77°10.084'	16:14	72	
M92-220	MUC 39	25.01.	12°13.531'	77°10.060'	16:36	71	*Inc (N-exp)*
M92-221	Glider	25.01.	12°15.72'	77°22.39'	18:00	154.4	
M92-222	Glider	25.01.	12°18.75'	77°26.77'	18:54	202.9	
M92-223	MUC 40	25.01.	12°35.385'	77°40.513'	21:24	1030	
M92-224	Profiler 5	25.01.	12°35.450'	77°41.158'	23:10	1019	Recovery
M92-225	CTD 62	25.01.	12°35.522'	77°41.058'	23:39	1028	Nutrients
M92-226	MSS 34	26.01.	12°35.451'	77°40.888'	00:59	1000	
M92-227	CTD/RO 63	26.01.	12°36.897'	77°41.259'	03:03	1103	
M92-228	MSS 35	26.01.	12°31.417'	77°35.203'	05:01	775	
M92-229	CTD/RO 64	26.01.	12°32.723'	77°35.554'	06:53	862	Nutrients
M92-230	MSS 36	26.01.	12°30.997'	77°34.706'	08:10	700	
M92-231	CTD/RO 65	26.01.	12°31.371'	77°35.223'	10:09	773	Nutrients
M92-232	BIGO-II-5	26.01.	12°27.22'	77°29.60'	13:00	410.6	Recovery
M92-233	Glider IFM 10	26.01.	12°24.202'	77°29.530'	13:42	340	
M92-234	MUC 41	26.01.	12°30.508'	77°33.975'	15:35	617	
M92-235	MUC 42	26.01.	12°30.754'	77°34.176'	16:40	648	Foraminiferal sands
M92-236	MUC 43	26.01.	12°30.757'	77°34.179'	17:40	646	Foramineferal sands *Inc (N-exp)*
M92-237	CTD 66	26.01.	12°30.757'	77°34.180'	18:31	648	
M92-238	MUC 44	26.01.	12°22.699'	77°29.100'	20:30	307	MUC for MPI *Inc (N-exp)*
M92-239	In situ pumps 18	26.01.	12°21.51'	77°21.70'	21:58	197.3	
M92-240	CTD 67	27.01.	12°14.692'	77°12.396'	02:08	98.8	
M92-241	CTD/RO 68	27.01.	12°13.126.'	77°10.215'	02:53	70	Nutrients
M92-242	MSS 37	27.01.	12°14.141'	77°11.650'	03:33	85	
M92-243	CTD/RO 69	27.01.	12°14.654'	77°11.862'	05:03	91	Nutrients
M92-244	MSS 38	27.01.	12°13.571'	77°10.323'	06:06	75	
M92-245	CTD/RO 70	27.01.	12°14.177'	77°10.501'	08:15	78	Nutrients
M92-246	MSS 39	27.01.	12°13.595'	77°10.332'	09:00	80	
M92-247	MUC 45	27.01.	12°21.492'	77°21.701'	12:55	194.8	

Station	Gear No.	Date	Position		Time	Depth	Remarks
No.		2013	Lat. [°S]	Long. [°W]	[UTC]	[m]	
M92-248	MUC 46	27.01.	12°16.697'	77°15.002	14:07	129	
M92-249	BIGO-I-5	27.01.	12°14.898'	77°12.705'	15:44	101	Deployment
M92-250	Glider IFM 03	27.01.	12°19.84'	77°26.24'	17:32	214.4	
M92-251	Profiler 6	27.01.	12°30.755'	77°34.175'	19:37	650	Deployment
M92-252	GC 1	27.01.	12°35.400'	77°40.493'	22:08	1031	35.31 kN tension; 75 cm core recovery; many carbonates and silty
M92-253	GC 2	27.01.	12°37.051'	77°43.635'	23:45	1121.7	41.88 kN max. tension; < 50 cm core
M92-254	GC 3	28.01.	12°27.191'	77°29.490'	02:00	407.2	30.34 kN max. tension
M92-255	GC 4	28.01.	10°59.995'	78°0.914'	13:01	188	28 kN tension
M92-256	CTD 71	28.01.	11°0.106'	78°0.958'	13:35	188.7	Nutrients
M92-257	CTD/RO 72	28.01.	10°59.991'	77°56.693'	14:39	150	Nutrients
M92-258	CTD 73	28.01.	10°59.999'	77°51.954'	15:34	117	Nutrients
M92-259	CTD/RO 74	28.01.	10°59.996'	77°47.410'	16:30	80	Nutrients
M92-260	CTD 75	28.01.	11°0.021'	78°5.287'	18:23	248	Nutrients
M92-261	CTD 76	28.01.	11°0.033'	78°12.669'	19:42	363	Nutrients
M92-262	GC 5	28.01.	10°59.999'	78°12.605'	20:25	366	26.1 kN
M92-263	GC 6	28.01.	10°59.998'	78°12.605'	21:03	361	25.43 kN
M92-264	CTD 77	28.01.	10°59.992'	78°15.307'	21:52	400	Nutrients
M92-265	GC 7	29.01.	10°59.989'	78°38.011'	00:18	1485	43.7 kN
M92-266	CTD/RO 78	29.01.	11°0.049'	78°38.018'	01:21	1500	Nutrients
M92-267	BIGO-I-5	29.01.	12°14.89'	77°12.79'	13:00	101.1	Recovery
M92-268	GC 8	29.01.	12°14.500'	77°9.611'	13:41	78	19.67 kN; 4m core
M92-269	CTD/RO 79	29.01.	12°16.690'	77°14.999'	14:39	128	
M92-270	GC 9	29.01.	12°23.276'	77°24.198'	16:15	243.2	17.38 kN; only 1m core retrieval; penetration with 0.3m/s
M92-271	GC 10	29.01.	12°23.294'	77°24.200'	16:47	243.6	18.23 kN; possibly fall over; only 1m core retrieval; penetration with 0.6 m/s
M92-272	GC 11	29.01.	12°23.299'	77°24.201'	17:21	243	17.77 kN; possibly fall over; penetration with 1.0 m/s; only 1m core; massive carbonates in core catcher
M92-273	GC 12	29.01.	12°23.327'	77°24.205'	17:46	243.8	19.83 kN; completely deployed with 1

Station	Gear No.	Date	Position		Time	Depth	Remarks
No.		2013	Lat. [°S]	Long. [°W]	[UTC]	[m]	
							m/s; only 1 m core
M92-274	GC 13	29.01.	12°23.353'	77°24.210'	18:14	244.7	20.01 kN; completely deployed with 1.5 m/s; core catcher slightly damaged; 1.5m core
M92-275	MSS 40	29.01.	12°20.744'	77°34.136'	19:54	645	
M92-276	CTD/RO 80	29.01.	12°31.345'	77°33.922'	20:58	680	Nutrients
M92-277	Profiler 6	29.01.	12°30.634'	77°34.233'	21:57		Recovery
M92-278	GoFlo 12	29.01.	12°21.5'	77°21.7'	23:45	195	
M92-279	CTD/RO 81	30.01.	12°21.490'	77°21.713'	00:52	195	
M92-280	MSS 41	30.01.	12°21.489'	77°21.713'	01:34	195	
M92-281	CTD/RO 82	30.01.	12°22.517'	77°21.065'	03:21	204	Nutrients
M92-282	In situ pumps 19	30.01.	13°9.897'	76°50.109'	12:00	253.5	
M92-283	CTD 83	30.01.	13°9.897'	76°50.110'	16:09	254	Nutrients
M92-284	MUC 47	30.01.	13°9.800'	76°50.127'	17:08	254	Mostly bare sand but patchy; Microbial mats
M92-285	In situ pumps 20	30.01.	13°9.90'	76°50.10'	17:52	255.1	
M92-286	MUC 48	30.01.	13°10.041'	76°58.889'	21:45	599	Sandy sediment; all cores are empty
M92-287	MUC 49	30.01.	13°10.203'	76°57.802'	23:06	501	
M92-288	CTD 84	31.01.	12°13.128'	77°10.215'	04:56	68	
M92-289	MUC 50	31.01.	10°59.997'	77°47.388'	13:07	83.1	

8 Data and Sample Storage and Availability

The data were collected within the Kiel Sonderforschungsbereich (SFB) 754. In Kiel a joint data management team of GEOMAR and Kiel University organizes and supervises data storage and publication by marine science projects in a web-based multi-user system. In a first phase data are only available to the project user groups. After a three year proprietary time the data management team will publish these data by dissemination to national and international data archives, i.e. the data will be submitted to PANGAEA no later than February, 2016. Digital object identifiers (DOIs) are automatically assigned to data sets archived in the PANGAEA Open Access library making them publically retrievable, citeable and reusable for the future. All metadata are immediately available publically via the following link pointing at the GEOMAR portal (https://portal.geomar.de/metadata/leg/show/316034).

In addition the portal provides a single downloadable KML formatted file (https://portal.geomar.de/metadata/leg/kmlexport/316034) which retrieves and combines up-to-date cruise (M92) related information, links to restricted data and to published data for visualisation e.g. in GoogleEarth.

The following data sets will become available: bathymetry; hydrological data from Glider, CTD casts, moorings, small sized satellite lander, and microstructure CTD; water column nutrient data and N-isotopes from CTD/water sampling rosette casts and GOFLO; water column and sediment radiotracer data from in situ pump, CTD casts and MUC deployments, porewater geochemistry from MUC, GC and BIGO Lander; in situ flux measurements from BIGO Lander; microbiological data from MUC, BIGO Lander and GC; in situ micro profiles for O_2, NO_3^-, and N_2O, sea floor video footage obtained during MUC deployments.

9 Acknowledgements

We like to thank captain Michael Schneider, his officers and crew of RV METEOR for their support of our scientific programme and for creating a very friendly and professional working atmosphere on board. The ship time of METEOR was provided by the German Science Foundation (DFG) within the core program METEOR/MERIAN. Financial support for the different projects carried out during the cruise was mostly provided though the collaborative research program SFB 754 (Climate – Biogeochemical interactions in the tropical Oceans) supported by the German Science Foundation (DFG). We are grateful for the participation of E. Johnston and J. Salazar from IMARPE (Peru), who performed own measurements and helped with the sampling. We like to thank also the authorities of Peru for their permission to carry out scientific work in their territorial waters.

10 References

Altabet, M.A., 2001. Nitrogen isotopic evidence for micronutrient control of fractional NO_3^- utilization in the equatorial pacific. Limnology and Oceanography 46 (2), 368-380.

Binnerup, S. J., Jensen, K., Revsbech, N. P., Jensen, M. H., Sørensen, J.,1992. Denitrification, dissimilatory reduction of nitrate to ammonium, and nitrification in a bioturbated estuarine sediment as measured with 15N and microsensor techniques, Appl. Environ. Microb., 58, 303–313.

Buesseler, K. O., Benitez-Nelson, C. R., Moran, S. B., Burd, A. B., Charette, M. A., Cochran, J. K., Coppola, L., Fisher, N. S., Fowler, S. W., Gardner, W., Guo, L. D., Gustafsson, O., Lamborg, C., Masque, P., Miquel, J. C., Passow, U., Santschi, P. H., Savoye, N., Stewart, G., Trull, T., 2006. An assessment of particulate organic carbon to thorium-234 ratios in the ocean and their impact on the application of Th-234 as a POC flux proxy, Mar. Chem., 100, 213-233, 10.1016/j.marchem.2005.10.013.

Bohlen, L., Dale, A. W., Sommer, S., Mosch, T., Hensen, C., Noffke, A., Scholz, F., Wallmann, K., 2011. Benthic nitrogen cycling traversing the Peruvian oxygen minimum zone. Geochimica et Cosmochimica Acta 75, 6094-6111.

Bourbonnais, A., Lehmann, M.F., Waniek, J.J., Schulz-Bull, D.E., 2009. Nitrate isotope anomalies reflect N_2 fixation in the Azores Front region (subtropical NE Atlantic). Journal of Geophysical Research 114 (C03003), doi:10.1029/2007JC004617.

Cacchione, D. A., Drake, D.E., 1986. Nepheloid layers an internal waves over continental shelves and slopes. Geo-Marine Letters 6, 147-152.

Capone, D. G., 1993. Determination of nitrogenase activity in aquatic sampes using the acetylene reduction procedure. In: Kemp, P. F., Sherr, B. F., Sherr, E. B., Coles J. J.

(Eds.), Handbook of methods in aquatic microbial ecology. Boca Raton: CRC Press LLC. pp. 621–631.

Cline, J.D., Kaplan, I.R., 1975. Isotopic fractionation of dissolved nitrate during denitrification in the eastern tropical north pacific ocean. Marine Chemistry 3 (4), 271-299.

Croot, P. L., Laan, P., 2002. Continuous shipboard determination of Fe (II) in polar waters using flow injection analysis with chemiluminescence detection, Anal. Chim. Acta, 466, 261–273.

Danielsson, L.-G., B. Magnusson, Westerlund, S., 1978. An improved metal extraction procedure for the determination of trace metals in sea water by atomic absorption spectrometry with electrothermal atomisation, Anal. Chim. Acta, 98, 47– 57.

Garrett, C., Gilbert, D., 1988. Estimates of vertical mixing by internal waves refelected off a sloping bottom. In: Nihoul, J.C.J., Jamart, B.M. (Eds) Smallscale turbulence and mixing in the ocean, Elsevier, pp. 405-423.

Glock, N., Schönfeld, J., Eisenhauer, A., Hensen, C., Mallon, J., Sommer, S., 2013. The role of benthic foraminifera in the benthic nitrogen cycle of the Peruvian oxygen minimum zone. Biogeosciences,10, 4767-4783.

Glud, R. N., Stahl, H., Berg, P., Wenzhofer, F., Oguri, K., Kitazato H., 2009. In situ microscale variation in distribution and consumption of O_2: A case study from a deep ocean margin sediment (Sagami Bay, Japan). Limnology and Oceanography 54(1), 1-12.

Gooday, A. J., Levin, L. A., Linke, P., Heeger, T. 1992 The role of benthic foraminifera in deep-sea food webs and carbon cycling. In: Rowe, G. T., Parient, V. (Eds) Deep-sea Food Chains and the global Carbon Cycle. Dordrecht, Kluwer.

Granger, J., Sigman, D.M., Lehmann, M.F., Tortell, P.D., 2008. Nitrogen and oxygen isotope fractionation during dissimilatory nitrate reduction by denitrifying bacteria. Limnology and Oceanography 53 (6), 2533-2545.

Holtappels, M., Lavik, G., Jensen, M. M., Kuypers, M. M. M., 2011. 15N-Labeling Experiments to Dissect the Contributions of Heterotrophic Denitrification and Anammox to Nitrogen Removal in the OMZ Waters of the Ocean. Methods in enzymology (1st ed., Vol. 486, pp. 223–251). Elsevier Inc. doi:10.1016/B978-0-12-381294-0.00006-7

Holloway, P.E., 1985. A comparison of semidiurnal internal tides from different bathymetric locations on the Australian north-west shelf. J. Phys. Oceanogr., 15, 240-251.

Jørgensen, B.B., 1978. A comparison of methods for the quantification of bacterial sulphate reduction in coastal marine sediments: I. Measurements with radiotracer techniques. Geomicrobiol. J. 1: 11-27

Knapp, A. N., Sigman, D. M., and Lipschultz, F., 2005. N isotopic composition of dissolved organic nitrogen and nitrate at the Bermuda Atlantic time-series Study site. Global Biogeochemical Cycles 19, GB1018, doi:10.1029/2004GB002320.

Koroleff, F., Kremling, K. 2007. Analysis by spectrophotometry. In: Grasshoff, K, Kremling, K, Ehrhardt M. (Eds.). Methods of seawater analysis, 3rd Ed., Wiley, DOI: 10.1002/9783527613984.

Ku, T.-L. Luo, S., 2008. Ocean Circulation/Mixing Studies with Decay-Series Isotopes. In: Krishnaswami, S. Cochran, J.K. (Eds), Radioactivity in the Environment. Elsevier, pp. 307-344.

McIlvin, M. R., Altabet, M. A. 2005. Chemical conversion of nitrate and nitrite to nitrous oxide for nitrogen and oxygen isotopic analysis in freshwater and seawater. Analytical Chemistry 77, 5589–5595.

McIlvin, M. M., Casciotti, K. L., 2010. Automated stable isotopic analysis of dissolved nitrous oxide at natural abundance levels. Limnology and Oceanography- Methods 8, 54–66.

Moore, W.S., 2008. Fifteen years' experience in measuring ^{224}Ra and ^{223}Ra by delayed – coincidence counting.

Mosch, T., Sommer, S., Dengler, M., Noffke, A., Bohlen, L., Pfannkuche, O., Liebetrau, V., Wallmann, K., 2012. Factors influencing the distribution of epibenthic megafauna acros the Peruvian oxygen minimum zone. Deep-Sea Research I, 68, 123-135.

Nielsen, L. P., 1992. Denitrification in sediment determined from nitrogen isotope pairing. FEMS Microbiology Letters 86(4), 357-362.

Noffke, A., Hensen, C., Sommer, S., Scholz, F., Bohlen, L., Mosch, T., Graco, M., Wallmann, K., 2012. Benthic iron and phosphorus fluxes across the Peruvian oxygen minimum zone. Limnology and Oceanography, 57, 851-867.

Noffke, A., Hensen, C., Dale, A. W., Sommer, S., Mosch, T., Bohlen, L., Wallmann, K., (in prep.) A missing source of phosphate in the sediment budget of the Peruvian oxygen minimum zone.

Phillips, O. M., 1977. The dynamics oft he upper ocean. 2nd edition, Cambridge University Press, New York, 336 pp.

Piña-Ochoa, E., Høgslund, S., Geslin, E., Cedhagen, T., Revsbech, N. P., Nielsen, L. P., et al., 2010. Widespread occurrence of nitrate storage and denitrification among Foraminifera and Gromiida. Proc Natl Acad Sci USA. 107, 1148–1153.

Pernthaler, A., Pernthaler, J., Amann, R., 2002. Fluorescence in situ hybridization and catalyzed reporter deposition for the identification of marine bacteria. Applied and environmental microbiology, 68(6), 3094–101.

Rathburn, A. E., Corliss, B. H., 1994. The ecology of living (stained) deep-sea benthic foraminifera from the Sulu Sea. Paleoceanography, 9, 87–150.

Revsbech, N. P., Christensen, P. B., Nielsen, L. P., Sørensen, J., 1989. Denitrification in a trickling filter biofilm studied by a microsensor for oxygen and nitrous oxide. Water Res., 23, 867–87.

Risgaard-Petersen, N., Langezaal, A. M., Ingvardsen, S., Schmid, M. C., Jetten, M. S. M., Op den Camp, H. J. M., et al., 2006. Evidence for complete denitrification in a benthic foraminifer. Nature, 443, 93–96.

Rutgers van der Loeff, M. M., Sarin, M. M., Baskaran, M., Benitez-Nelson, C. R., Buesseler, K. O., Charette, M. A., Dai, M., Gustafsson, O., Masque, P., Morris, P. J., Orlandini, K., Rodriguez y Baena, A. M., Savoye, N., Schmidt, S., Turnewitsch, R., Voge, I., Waples, J. T., 2006. A review of present techniques and methodological advances in analyzing Th-234 in aquatic systems, Mar. Chem., 100, 190-212.

Sigman, D. M., Casciotti, K. L., Andreani, M., Barford, C., Galanter, M., and Bohlke, J. K. 2001. A bacterial method for the nitrogen isotopic analysis of nitrate in seawater and freshwater. Analytical Chemistry 73, 4145–4153.

Sigman, D.M., Granger, J., DiFiore, P.J., Lehmann, M.M., Ho, R., Cane, G., van Geen, A., 2005. Coupled nitrogen and oxygen isotope measurements of nitrate along the eastern North Pacific margin. Global Biogeochemical Cycles 19 (4).

Sommer, S., P. Linke, O. Pfannkuche, T. Schleicher, J. Schneider v. Deimling, A. Reitz, M. Haeckel, S. Flögel, Hensen, C., 2009. Seabed methane emissions and the habitat of frenulate tubeworms on the Captain Arutyunov mud volcano (Gulf of Cadiz), Mar. Ecol. Prog. Ser., 382, 69–86, doi: 10.3354/meps07956.

Sørensen, J., 1978. Denitrification rates in a marine sediment as measured by the acetylene inhibition technique, Appl. Environ. Microb., 36, 139–143.

Thamdrup, B., Dalsgaard, T., 2002. Production of N-2 through anaerobic ammonium oxidation coupled to nitrate reduction in marine sediments." Applied and Environmental Microbiology, 68(3), 1312-1318.

Vandieken, V., Nickel, M., Jørgensen, B.B., 2006. Carbon mineralization in Arctic sediments northeast of Svalbard: Mn(IV) and Fe(III) reduction as principal anaerobic respiratory pathways. Mar. Ecol. Prog. Ser. 322: 15-27

Welsh, D. T., Bourgues, S., Wit, R. De, Herbert, R. A., 1996. Seasonal variations in nitrogen-fixation (acetylene reduction) and sulphate-reduction rates in the rhizosphere of Zostera noltii: nitrogen fixation by sulphate-reducing bacteria. Marine Biology, 125, 619–628.

Yoshida, N., Toyoda, S., 2000. Constraining the atmospheric N_2O budget from intramolecular site preference in N_2O isotopomers. Nature 405, 330–334.

Yoshinari, T., Altabet, M. A., Naqvi, S. W. A., Codispoti, L., Jayakumar, A., Kuhland, M., Devol, A., 1997. Nitrogen and oxygen isotopic composition of N_2O from suboxic waters of the eastern tropical North Pacific and the Arabian Sea – Measurements by continuous-flow isotope ratio monitoring. Marine Chemistry 56(3–4), 253–264.

Zhang, L., Altabet, M. A., Wu, T., Hadas, O., 2007. Sensitive measurement of NH_4 $^{15}N/^{14}N$ ($^{15}NH_4$) at natural abundance levels in fresh and saltwaters. Analytical Chemistry 79, 5297–5303.